

# LAP<sub>2</sub>: Revisiting Laplace DP-SGD for High Dimensions via Majorization Theory

Meisam Mohammady<sup>†</sup>, Qin Yang<sup>¶</sup>, Nicholas Stout<sup>†</sup>, Ayesha Samreen<sup>†</sup>, Han Wang<sup>§</sup>,  
Christopher J Quinn<sup>†</sup>, Yuan Hong<sup>¶</sup>

<sup>†</sup>Iowa State University, <sup>¶</sup>University of Connecticut, <sup>§</sup>University of Kansas

**Abstract**—Differentially Private Stochastic Gradient Descent (DP-SGD) is a cornerstone technique for ensuring privacy in deep learning, widely used in both training from scratch and fine-tuning large-scale language models. While DP-SGD predominantly relies on the Gaussian mechanism, the Laplace mechanism remains underutilized due to its reliance on  $\ell_1$  norm clipping. This constraint severely limits its practicality in high-dimensional models because the  $\ell_1$  norm of an  $n$ -dimensional gradient can be up to  $\sqrt{n}$  times larger than its  $\ell_2$  norm. As a result, the required noise scale, and thus the privacy loss, grows significantly with model size, leading to poor utility or untrainable models.

In this work, we introduce LAP<sub>2</sub>, a new solution that enables  $\ell_2$  clipping for Laplace DP-SGD while preserving strong privacy guarantees. We overcome the dimensionality-driven clipping barrier, by computing coordinate-wise moment bounds and applying *majorization theory* to construct a tight, data-independent upper bound over the full model. By exploiting the *Schur-convexity* of the moment accountant function, we aggregate these bounds using a carefully designed majorization set that respects the  $\ell_2$  clipping constraint. This yields a multivariate privacy accountant that scales gracefully with model dimension and enables the use of thousands of moments. Empirical evaluations demonstrate that our approach significantly improves the performance of Laplace DP-SGD, achieving results comparable to or better than Gaussian DP-SGD under strong privacy constraints. For instance, fine-tuning RoBERTa-base (125M parameters) on SST-2 achieves 87.88% accuracy at  $\epsilon = 0.54$ , outperforming Gaussian (87.16%) and standard Laplace (48.97%) under the same budget.

**Index Terms**—Differential Privacy, DP-SGD, Laplace, Majorization Theory

## I. INTRODUCTION

Training and fine-tuning deep learning models pose significant privacy risks. During training, adversaries can exploit gradient updates, model outputs, and pre-trained parameters to reconstruct sensitive data, making privacy a critical concern. Moreover, fine-tuning large pre-trained language models, such as BERT [1] and GPT families [2], is essential for achieving state-of-the-art performance in various tasks, including sentence classification [1], text generation [3], and code generation [4]. Data reconstruction attacks, such as Updates-Leak [5] and Inverting Gradients [6], achieve success rates of up to 80%, while the Dynamic Memory Model Inversion Attack (DMMIA) [7] enhances realism, reaching 93.54% on FaceScrub. Additionally, prompt-based techniques further expose LLMs to training data extraction attacks, increasing the risk of recovering individual samples [8].

To mitigate privacy risks during model training and fine-tuning, differential privacy (DP) [9] has become the de facto

privacy model. A widely adopted method, Differentially Private Stochastic Gradient Descent (DP-SGD) [10], provides DP guarantees by ensuring that the inclusion or exclusion of any single data sample does not significantly impact the model’s output. DP-SGD achieves this by clipping gradients to limit the influence of individual samples and adding Gaussian noise to the gradients within each batch. While DP-SGD effectively controls the privacy budget consumed over the thousands of iterations typically required for model training or fine-tuning, it often results in noticeable utility loss [10], [11], [12].

However, Gaussian noise exhibits the *privacy wall* phenomenon [13], [14], where DP-SGD with Gaussian perturbations fails to attain the optimal privacy–utility scaling  $\sigma = \Theta(1/\epsilon)$  in the medium privacy regime, resulting in suboptimal trade-offs. This occurs because the moments accounting function (MAF) for Gaussian noise follows a quadratic exponential form, causing accounted privacy loss to escalate rapidly as  $\lambda$  increases. Then, Gaussian-based DP-SGD may degrade model accuracy and slow convergence to some extent, particularly in **high-privacy regimes** (small  $\epsilon$ ).

Alternatively, Laplace mechanism [15] has been shown to preserve accuracy better than the Gaussian mechanism in stricter privacy regimes, particularly in low-dimensional settings [16], [17]. This advantage could be highly beneficial for deep learning, by ensuring strong privacy guarantees across many training iterations. However, this improvement has not been fully realized, likely due to the destructive impact of  $\ell_1$ -norm clipping in high-dimensional spaces (DP-SGD with Laplace mechanism requires it by default). This limitation arises because, for an  $n$ -dimensional gradient vector, the  $\ell_1$  norm can be up to  $\sqrt{n}$  times larger than its  $\ell_2$  norm.

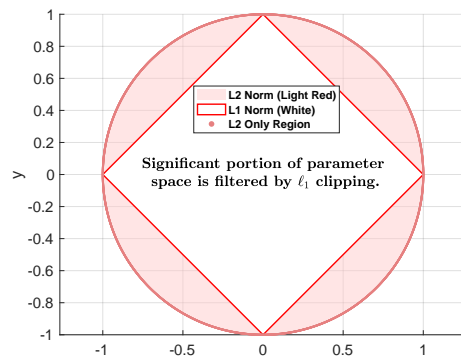


Fig. 1: Comparison of  $\ell_1$  and  $\ell_2$  norm clipped spaces.

Both the Laplace and Gaussian mechanisms can be applied to vector-valued functions, but they differ fundamentally in how they interact with gradient clipping. The Gaussian mechanism is based on  $\ell_2$  sensitivity and is naturally compatible with  $\ell_2$  norm clipping, preserving a large feasible region for optimization—especially in high-dimensional settings. In contrast, the Laplace mechanism requires  $\ell_1$  norm clipping due to its dependence on  $\ell_1$  sensitivity. As illustrated in Figure 1, this severely restricts the optimization region and leads to overly conservative updates, often degrading training performance under strong privacy constraints.

To resolve this mismatch, we propose a new privacy accounting framework for Laplace DP-SGD that supports  $\ell_2$  norm clipping. A natural workaround (summing coordinate-wise privacy losses) can be overly pessimistic in high-dimensional settings, as it ignores the global  $\ell_2$  constraint and accumulates leakage too conservatively.

Our key insight is to instead apply *majorization theory* [18], a classical tool from inequality analysis, to derive a tighter, dimension-aware privacy bound. When the moments accountant is *Schur-convex*, as in the case of the Laplace mechanism, we can replace the actual vector of per-parameter gradient magnitudes with a carefully constructed *majorization set*, a worst-case configuration that dominates all valid  $\ell_2$ -clipped gradients. This allows us to compute moment bounds for each coordinate and sum them over the majorization set instead of the data-dependent gradients.

This yields a tight, dimension-aware upper bound on privacy loss that remains data-independent and scales gracefully with model size. As a result, our method, LAP<sub>2</sub>, enables high-utility training of large models such as RoBERTa-Large and ViT under strong privacy budgets (e.g.,  $\epsilon \leq 1$ ), making the Laplace mechanism a practical choice once again for modern DP-SGD workloads.

Beyond the theoretical contributions, we introduce a framework that enables practitioners to integrate LAP<sub>2</sub> into various AI applications by adapting noise parameters to task-specific needs. Our framework allows users to systematically compute the optimal Laplace noise scale ( $b$ ) and clipping parameter ( $C$ ) based on: (1) AI task specifications (epochs, batch size, model size), and (2) DP constraints ( $\epsilon, \delta$ ).

Therefore, the main contributions are summarized as below:

- 1) Taking the first step to advance the *Laplace mechanism in DP-SGD* by mitigating its reliance on  $\ell_1$  clipping through *majorization theory*, enabling tighter privacy accounting under fixed distortion.
- 2) Introducing LAP<sub>2</sub> that offers *plug-and-play DP-SGD* where users can seamlessly compute optimal clipping and noise parameters for their setups.
- 3) Theoretically analyzing LAP<sub>2</sub>'s privacy and performance, and comprehensively comparing the LAP<sub>2</sub> and *Gaussian* mechanisms in DP-SGD.
- 4) Conducting comprehensive empirical evaluations on both vision and language models, demonstrating that LAP<sub>2</sub> consistently performs comparably to the Gaussian

mechanism, with higher accuracy in certain strong-privacy regimes and larger model fine-tuning.

Our evaluation code and additional experimental results are publicly available at [the LAP<sub>2</sub> evaluation repository](#).

## II. PRELIMINARIES

We review some background on differential privacy and DP-SGD for the theoretical foundations of the LAP<sub>2</sub> framework.

### A. Differential Privacy

Differential privacy ensures individual input privacy by introducing randomness into the output, either by injecting explicit noise or by leveraging inherent stochasticity in the mechanism or inputs<sup>1</sup>. Let  $\mathcal{D}$  denote the space of datasets of interest. A mechanism can be viewed as a probabilistic algorithm designed to answer a query  $q$ , which is a map  $q : \mathcal{D} \rightarrow \mathbb{R}^n$ . We sometimes index the mechanism by the query  $q$  of interest, denoting it as  $M_q$ . In particular, we denote mechanisms answering queries  $q : \mathcal{D} \rightarrow \mathbb{R}$  by  $M_q(\mathcal{D})$ . Additionally, we define a symmetric binary relation, Adj, on  $\mathcal{D}$ , called *adjacency* [19]. Two datasets  $d \in \mathcal{D}$  and  $d' \in \mathcal{D}$  are adjacent, denoted Adj( $d, d'$ ), if and only if they differ by the data of a single participant. The standard definitions of differential privacy introduced in [20], [21] will follow.

**Definition II.1** (Differential Privacy [22]). A randomization mechanism  $M_q : \mathcal{D} \times \Omega \rightarrow \mathbb{R}^n$  which is  $\epsilon$ -differentially private, necessarily randomizes its output in such a way that for all adjacent datasets  $d, d' \in \mathcal{D}$  and  $S \in \mathbb{R}^n$ ,

$$\mathbb{P}(M_q(d) \in S) \leq e^\epsilon \mathbb{P}(M_q(d') \in S). \quad (\text{II.1})$$

If the inequality fails, an  $\epsilon$ -breach occurs, indicating a non-negligible probability to distinguish the presence or absence of any single  $d_n = d - d'$ . The following norms will be frequently used throughout the remainder of the paper.

**Definition II.2.** The  $\ell_1$  and  $\ell_2$  norms of a vector  $x \in \mathbb{R}^n$  are defined as:  $\|x\|_1 = \sum_{i=1}^n |x_i|$ ,  $\|x\|_2 = (\sum_{i=1}^n x_i^2)^{\frac{1}{2}}$  where  $x = (x_1, x_2, \dots, x_n)$  is a vector in  $\mathbb{R}^n$ .

We now recall a fundamental mechanism that provides  $\epsilon$ -differential privacy when answering queries.

**Definition II.3** (Laplace Mechanism [23]). Given a numerical query  $q(d)$  (whose output lies in  $\mathbb{R}^n$ ) and a scale  $b$ , the Laplace mechanism  $M_q(d, b)$  modifies  $q(d)$  by adding noise  $w \sim \text{Lap}(b)$ , i.e.,  $M_q(d, b) = q(d) + w$ .

Recall that the (univariate) Laplace distribution with mean zero and scale  $b$ , denoted  $\text{Lap}(b)$ , has density  $p(x; b) = \frac{1}{2b} \exp(-|x|/b)$  and variance  $2b^2$ . For  $w \in \mathbb{R}^n$  with i.i.d. components  $w_i \sim \text{Lap}(b)$ , the joint density is  $(\frac{1}{2b})^n \exp(-\|w\|_1/b)$  and  $\|\cdot\|_1$  denotes the  $\ell_1$  norm [24].

The scale parameter in the Laplace mechanism determines the degree of privacy. Specifically:

<sup>1</sup>Developing a unified framework to capture all randomness sources and translate them into differential privacy guarantees remains an open challenge [13]. Here, we assume a fixed probability space  $(\Omega, \mathcal{F}, P)$ , where  $\Omega$  is the sample space,  $\mathcal{F}$  is a  $\sigma$ -algebra of events, and  $P$  is the probability measure.

**Theorem II.4** (Laplace Mechanism [25]). Let  $q : \mathcal{D} \rightarrow \mathbb{R}$  be a query with (global)  $\ell_1$ -sensitivity  $\Delta_1 q = \max_{d, d' : \text{Adj}(d, d')} \|q(d) - q(d')\|_1$ . If the Laplace mechanism  $M_q(d, b)$  uses a scale parameter  $b \geq \frac{\Delta_1 q}{\epsilon}$ , then  $M_q(d, b)$  is  $\epsilon$ -differentially private.

Following the introduction of differential privacy [21], [22], various relaxations were proposed to capture the properties of Gaussian additive noise. Among these, approximate DP introduced an additive  $\delta$  term for Gaussian noise analyses which is typically of the order of  $\frac{1}{|\mathcal{D}|}$ .

**Definition II.5** (Approximate Differential Privacy [19]). A randomization mechanism  $M_q : \mathcal{D} \rightarrow \mathcal{R}$  is said to provide  $(\epsilon, \delta)$ -DP for releasing the query results  $q(\mathcal{D})$  if it randomizes its output such that, for any two adjacent datasets  $d, d' \in \mathcal{D}$  and all subsets  $S \subseteq \mathbb{R}^n$ , the following holds:

$$\mathbb{P}(M_q(d) \in S) \leq e^\epsilon \mathbb{P}(M_q(d') \in S) + \delta, \quad (\text{II.2})$$

where  $\delta$  represents the failure probability of the  $\epsilon$ -DP guarantee provided by the randomization mechanism.

**Definition II.6** (Gaussian Mechanism [19]). The Gaussian mechanism  $M_q(d, \sigma)$  modifies the answers to query  $q$  in the dataset  $d$  by adding noise  $w \sim \mathcal{N}(0, \sigma^2 \mathbf{I}_n)$ , that is,  $M_q(d, \sigma) = q(d) + w$ .

The Gaussian mechanism ensures approximate differential privacy. In particular, for  $\epsilon < 1$ , its standard deviation is given by  $\sigma = \frac{\Delta_2 q}{\epsilon} \sqrt{2 \ln(\frac{1.25}{\delta})}$ , where  $\Delta_2 q$  is the  $\ell_2$ -sensitivity of the query  $q$  across all adjacent datasets.

Sequentially applying DP mechanisms increases the overall privacy cost, as shown by various composition theorems [26], [27]. Naive composition states that chaining  $k$  mechanisms, each  $(\epsilon, \delta)$ -DP, results in an overall  $(k\epsilon, k\delta)$ -DP guarantee, which can be overly conservative. Stronger composition theorems, such as the *advanced composition* theorem [28], provide tighter bounds. In particular, the overall DP guarantee can become  $(\epsilon \sqrt{2k \ln(\frac{1}{\delta})} + k\epsilon(e^\epsilon - 1))$ .

### B. Deep Learning with Differential Privacy

DP-SGD [10] is the first method that integrates the guarantees of differential privacy (DP) into deep neural network (DNN) training. At each iteration  $t$ , the gradient  $\mathbf{g}_t(\mathbf{x})$  for a data point  $\mathbf{x}$  is clipped using a threshold  $C$ . Formally, the clipped gradient is defined as:

$$\mathbf{g}_C(\mathbf{x}) = \frac{\mathbf{g}_t(\mathbf{x})}{\max\left(1, \frac{\|\mathbf{g}_t(\mathbf{x})\|_2}{C}\right)}.$$

This clipping step ensures that the sensitivity of each gradient is bounded with respect to the inclusion of individual samples in the training set, thereby preparing it for the perturbation with a Gaussian mechanism.

$$\tilde{\mathbf{g}}(\mathbf{x}) = \mathbf{g}_C(\mathbf{x}) + \mathcal{N}(0, C^2 \sigma^2 \mathbf{I}_n). \quad (\text{II.3})$$

The final update  $\tilde{\mathbf{g}}$  is computed by averaging  $\tilde{\mathbf{g}}(\mathbf{x})$  over the batch of size  $L$ . Even with tighter composition bounds, training

over many iterations (e.g., thousands of rounds) can lead to high cumulative privacy loss ( $\epsilon$ ). DP-SGD mitigates this by formulating an accounting function over the privacy loss terms across rounds, namely the *Moments Accountant Function*. Consequently, DP-SGD with moments accounting achieves a significantly improved bound of  $\mathcal{O}(\epsilon \sqrt{TL}/|\mathcal{D}|, \delta)$ -DP.

**Moments Accounting Function.** Consider two neighboring datasets  $d, d' \in \mathcal{D}$  and an outcome  $o \in \mathbb{R}^n$  from the sanitized gradients  $\tilde{\mathbf{g}}(\cdot)$ . The *privacy loss* w.r.t.  $o$  is defined by

$$c(o; \text{aux}, d, d') = \log \left[ \frac{\mathbb{P}(\tilde{\mathbf{g}}(\text{aux}, d) = o)}{\mathbb{P}(\tilde{\mathbf{g}}(\text{aux}, d') = o)} \right]. \quad (\text{II.4})$$

DP-SGD ensures privacy by focusing on orthogonal updates relative to the ‘‘aux’’ state, which represents the model’s state **prior to** training on a specific data instance  $x_{i < N}$ . This instance has been sequentially updated through the iterative application of differentially private mechanisms [10].

Let  $\mu_0$  denote the probability density function (pdf) of  $\mathcal{N}(0, \sigma^2)$ , and  $\mu_1$  denote the pdf of  $\mathcal{N}(1, \sigma^2)$ . Let  $\mu$  denote the mixture of two Gaussians,  $\mu = (1 - \zeta)\mu_0 + \zeta\mu_1$ , where  $\zeta = L/\max\{d, d'\}$  denotes the batch sampling rate. Clipping with threshold  $C = 1$ , the privacy loss of DP-SGD with Gaussian noise is bounded [10] by:

$$c(o; \text{aux}, d, d') \leq \log \left[ \max \left\{ \frac{\mu_0(o)}{\mu(o)}, \frac{\mu_1(o)}{\mu(o)} \right\} \right]. \quad (\text{II.5})$$

DP-SGD separates clipping from privacy accounting. To incorporate the impact of the clipping parameter  $C$ , DP-SGD scales the Gaussian noise’s variance by  $C^2$  per Equation II.3 after accounting, without directly influencing privacy accounting itself. To bound the privacy loss more tightly, the moments of the random variable associated with  $c(o; \text{aux}, d, d')$  are tightly calculated and bounded. Precisely, for  $\lambda > 0$ , define

$$\alpha_M(\lambda; \text{aux}, d, d') = \log \mathbb{E}_{o \sim M(\text{aux}, d)} [\exp(\lambda c(o; \text{aux}, d, d'))]. \quad (\text{II.6})$$

We then take the worst-case over  $\text{aux}, d, d'$ :

$$\alpha_M(\lambda) = \max_{\text{aux}, d, d'} (\alpha_M(\lambda; \text{aux}, d, d')). \quad (\text{II.7})$$

Key properties of this *Moments Accounting Function (MAF)* include [10]:

1) **Composability.** For a sequence of adaptive mechanisms  $M_1, \dots, M_t$ ,

$$\alpha_{M_1, \dots, M_t}(\lambda) \leq \sum_{i=1}^t \alpha_{M_i}(\lambda). \quad (\text{II.8})$$

2) **Tail Bound.** For any  $\epsilon > 0$ , a sequence of adaptive mechanisms  $M_1, \dots, M_t$  is jointly  $(\epsilon, \delta)$ -DP for

$$\delta = \min_{\lambda > 0} \left( \exp(\alpha_{M_1, \dots, M_t}(\lambda) - \lambda \epsilon) \right). \quad (\text{II.9})$$

**Privacy Amplification with Subsampling.** While the MAF significantly tightens the privacy budget, DP-SGD’s main

strength arises from *privacy amplification via random sampling*, where the privacy cost per evaluation decreases *quadratically*—rather than linearly—with the sampling rate  $\zeta = \frac{L}{|d|}$ . For instance, Bun et al. [29] showed that  $\alpha(\lambda) \propto \zeta^2 \frac{6\lambda}{\sigma^2}$ . Mironov et al. [13] (Section 3.3) presented a tighter privacy amplification bound, which remains the state-of-the-art for the subsampled Gaussian mechanism. The bound is expressed as:

$$\alpha_{M_1, \dots, M_t}(\lambda) \leq t \cdot \log \sum_{\eta=0}^{\lambda+1} \binom{\lambda}{\eta} (1-\zeta)^{\lambda+1-\eta} \zeta^\eta \cdot \exp\left(\frac{\eta^2 - \eta}{2\sigma^2}\right). \quad (\text{II.10})$$

The final  $(\epsilon, \delta)$ -DP guarantee is derived using the tight conversion formula provided by Balle et al. [30]:

$$\epsilon(\delta) = \min_{\lambda > 0} \left( \frac{\alpha_{M_1, \dots, M_t}(\lambda)}{\lambda} + \log\left(\frac{\lambda}{\lambda+1}\right) - \frac{\log(\delta) + \log(\lambda+1)}{\lambda} \right).$$

This significantly enhances the analysis of privacy loss in scenarios involving repeated subsampling and Gaussian noise.

### III. PROBLEM STATEMENT

DP-SGD predominantly relies on the Gaussian mechanism, with Laplace noise only applied in limited cases [31], [32]. The fundamental limitation of the Laplace mechanism in these settings stems from its privacy loss, which requires  $\ell_1$ -clipping. This clips gradients more aggressively than  $\ell_2$ -clipping, especially in higher dimensions, resulting in less informative updates and making it less suitable for DP-SGD.

To formalize this difference, consider the well-known relationship between  $\ell_1$  and  $\ell_2$  norms:  $\|x\|_1 \leq \sqrt{n}\|x\|_2$ , which follows from the Cauchy–Schwarz inequality [33]. The difference in retained volume after  $C$ - $\ell_1$  vs.  $C$ - $\ell_2$  clipping corresponds to the ratio of the respective clipped spaces in  $\mathbb{R}^n$ : a cross-polytope with volume  $V_{\ell_1}(n, C) = \frac{(2C)^n}{n!}$  and a Euclidean ball with volume  $V_{\ell_2}(n, C) = \frac{\pi^{n/2} C^n}{\Gamma(n/2+1)}$ . Their ratio simplifies to

$$\frac{V_{\ell_1}(n, C)}{V_{\ell_2}(n, C)} = \left(\frac{2}{\sqrt{\pi}}\right)^n \frac{(n/2)!}{n!},$$

which shrinks exponentially as  $n$  increases, highlighting the severe loss of preserved vectors under  $\ell_1$  clipping.

Figure 2 depicts the volume differences between  $C$ - $\ell_1$  and  $C$ - $\ell_2$  norm balls across increasing dimensionality. As the number of model parameters  $n$  increases, these volumes diverge at an astronomical rate, making  $\ell_1$  clipping significantly more restrictive than  $\ell_2$  clipping in high dimensions by discarding a much larger proportion of gradients. Even with larger clipping thresholds, this geometric gap remains substantial for  $n > 20$ .

This geometric bottleneck directly impacts the applicability of the Laplace mechanism for deep learning with DP. When coupled with  $\ell_1$ -norm clipping, the mechanism confines updates to a cross-polytope whose volume decays exponentially with  $n$ , making it unsuitable for high-dimensional gradients.

We formalize the privacy loss induced under this setup.

**Theorem III.1** (Privacy Loss of a Laplace Mechanism). *The privacy loss of a Laplace mechanism with scale parameter  $b$ ,*

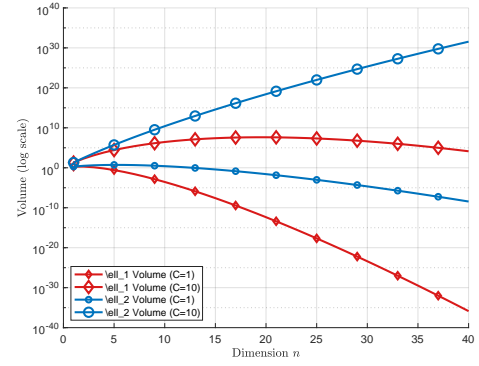


Fig. 2: Volume of  $n$ -dimensional vector space clipped by  $C$ - $\ell_1$  and  $C$ - $\ell_2$  norms.

applied to gradients clipped under the  $\ell_1$  norm with threshold  $C$ , is bounded by  $c(o; \text{aux}, d, d', b) \leq \frac{C}{b}$ .

*Proof.* Let  $\tilde{\mathbf{g}}(\text{aux}, \mathbf{x}, b)$  denote the output of a Laplace mechanism with scale  $b$ . The privacy loss at an outcome  $o$  is defined as:

$$c(o; \text{aux}, d, d', b) = \log \frac{\Pr[\tilde{\mathbf{g}}(\text{aux}, \mathbf{x}, b) = o]}{\Pr[\tilde{\mathbf{g}}(\text{aux}, -, b) = o]}, \quad (\text{III.1})$$

where  $\tilde{\mathbf{g}}(\text{aux}, -, b)$  denotes the outcome of the mechanism without access to the input  $\mathbf{x}$  (e.g.  $\mathbf{x}$  is only in one data set). Thus, without loss of generality, the denominator follows a zero-mean Laplace PDF, as in the worst-case setting it lacks any gradient component in direction of  $\mathbf{g}_C$ , while the numerator is centered around  $\mathbf{g}_C$ .

$$\begin{aligned} c(o; \text{aux}, d, d', b) &= \log \frac{\text{Lap}(\mathbf{g}_C(\mathbf{x}), bI_n)}{\text{Lap}(0, bI_n)} \\ &= \log \frac{\left(\frac{1}{2b}\right)^n \exp\left(-\frac{\|o - \mathbf{g}_C(\mathbf{x})\|_1}{b}\right)}{\left(\frac{1}{2b}\right)^n \exp\left(-\frac{\|o\|_1}{b}\right)} = \frac{\|o\|_1 - \|o - \mathbf{g}_C(\mathbf{x})\|_1}{b}. \end{aligned}$$

For all real valued vectors  $A$  and  $B$ , using  $\|A\|_1 = \|(A - B) + B\|_1$ , by the triangle inequality we have:  $\|A\|_1 - \|B\|_1 \leq \|A - B\|_1$ . Thus,

$$\frac{\|o\|_1 - \|o - \mathbf{g}_C(\mathbf{x})\|_1}{b} \leq \frac{\|\mathbf{g}_C(\mathbf{x})\|_1}{b} \quad (\text{III.2})$$

Evaluating the  $\ell_1$  norm in terms of the elements of  $\mathbf{g}_C(\mathbf{x}) = [\mathbf{g}_1, \mathbf{g}_2, \dots, \mathbf{g}_n]$ , we have:

$$c(o; \text{aux}, d, d', b) \leq \frac{\sum_{j=0}^n |\mathbf{g}_j|}{b}. \quad (\text{III.3})$$

Thus, this completes the proof.  $\square$

While  $c(o; \text{aux}, d, d', b) \leq \frac{C}{b}$  ensures bounded loss under  $\ell_1$ -clipping, applying it to gradients originally bounded in  $\ell_2$  (e.g.,  $\|x\|_2 \leq C$ ) requires using the inequality  $\|x\|_1 \leq \sqrt{n}\|x\|_2$ . This inflates the effective  $\ell_1$  clipping threshold to  $\sqrt{n}C$ , thereby scaling the privacy loss as  $\frac{\sqrt{n}C}{b}$ . As a result, naively using Laplace noise on  $\ell_2$ -clipped gradients leads to privacy degradation proportional to  $\sqrt{n}$ .

Thus, we pose the following problem.

## Problem Statement

Can we design a Laplace-based mechanism  $\mathcal{M}$  that operates over  $\ell_2$ -clipped vectors, i.e.,  $x \in \mathbb{R}^n$  with  $\|x\|_2 \leq C$ , while avoiding the  $\sqrt{n}$  privacy cost overhead induced by  $\|x\|_1 \leq \sqrt{n}\|x\|_2$ ?

That is, can

$$\mathcal{M}(x) \sim \text{Lap}_{B_2(C)}(x)$$

achieve strong  $(\epsilon, \delta)$ -privacy without worst-case  $\sqrt{n}$  degradation?

### A. DP-SGD with a LAP<sub>2</sub> Mechanism

To address the dimensional sensitivity problem stated earlier, we first present the moments accountant function for a subsampled uni-variate Laplace mechanism—where  $\ell_1$  and  $\ell_2$  clipping behave similarly at the coordinate level.

See Appendix A-A for the proof.

**Theorem III.2** (Subsampled Uni-variate Laplace Mechanisms). *Let  $M$  be a uni-variate Laplace mechanism with scale parameter  $b$  and sampling probability  $\zeta = \frac{L}{N}$ , where  $L$  is the mini-batch size and  $N$  is the dataset size. Suppose  $M$  is applied to a single partial derivative query (i.e. with respect to a single model parameter)  $q(d) = \mathbf{g}(d)$  clipped by threshold  $C$ , i.e.,  $|\mathbf{g}| \leq C$ .*

*Then, the moments accountant function of  $M_q$  satisfies*

$$\alpha_{M_q}(\lambda) = \log \left[ \sum_{\eta=0}^{\lambda+1} \binom{\lambda+1}{\eta} (1-\zeta)^{\lambda+1-\eta} \zeta^\eta F(C, \eta) \right], \quad (\text{III.4})$$

where

$$F(C, \eta) = \frac{\eta e^{\frac{(\eta-1)C}{b}} + (\eta-1)e^{-\frac{\eta C}{b}}}{2\eta-1}. \quad (\text{III.5})$$

While the uni-variate analysis in Equation III.4 provides an exact expression for each parameter, directly summing over millions of parameters can still lead to significant overestimation of the total privacy loss unless a tight holistic (multi-variate) bound is applied.<sup>2</sup>

To address this overestimation, we apply *Majorization Theory* [18], [34], a powerful tool for comparing vectors based on their spread or concentration. After  $\ell_2$  clipping with threshold  $C$ , the marginal clipped gradients  $|\mathbf{g}_i|$  are mostly small but unevenly distributed. To capture this structure, we construct a *majorization set*—a specially ordered vector that dominates the original gradient vector in a formal sense.

This majorization set enables us to bound any Schur-convex function of the original gradients by its value on the majorization set. Since the moments accountant function depends on the gradients through a Schur-convex structure, applying majorization allows us to obtain a tight holistic (multi-variate) privacy bound for  $\ell_2$ -clipped gradients.

<sup>2</sup>Here, the summation is over model parameters rather than training/fine-tuning iterations, similar to how composability traditionally applies over iterations. For the overall training/fine-tuning process, we would also need to compose over iterations.

In what follows, we first introduce background on majorization theory, then show that the moments accountant function given in Equation III.4 is Schur-convex. Finally, we derive a tight majorization set and use it to bound the total moment accountant function for Laplace mechanisms.

**Definition III.3** (Weak Majorization). Let  $\mathbf{x}, \mathbf{y} \in \mathbb{R}^n$ . We say that  $\mathbf{x}$  *weakly majorizes*  $\mathbf{y}$  from below, denoted  $\mathbf{x} \succ_w \mathbf{y}$ , if

$$\sum_{i=1}^k x_i^\downarrow \geq \sum_{i=1}^k y_i^\downarrow \quad \text{for all } k = 1, \dots, n,$$

where  $x_i^\downarrow$  and  $y_i^\downarrow$  denote the components of  $\mathbf{x}$  and  $\mathbf{y}$ , sorted in non-increasing order [18].

**Definition III.4** (Strong Majorization and Schur-Convexity). Let  $\mathbf{x}, \mathbf{y} \in \mathbb{R}^n$ . We say that  $\mathbf{x}$  is *majorized* by  $\mathbf{y}$ , denoted  $\mathbf{x} \prec \mathbf{y}$ , if

$$\sum_{i=1}^k x_i^\downarrow \leq \sum_{i=1}^k y_i^\downarrow \quad \text{for all } k = 1, \dots, n, \quad \text{and} \quad \sum_{i=1}^n x_i = \sum_{i=1}^n y_i.$$

A function  $F : \mathbb{R}^n \rightarrow \mathbb{R}$  is called *Schur-convex* if

$$\mathbf{x} \prec \mathbf{y} \quad \Rightarrow \quad F(\mathbf{x}) \leq F(\mathbf{y}).$$

Schur-convex functions favor vectors that are more spread out, making them useful for bounding symmetric functionals.

**Schur–Ostrowski Criterion** [35]. Let  $f : \mathbb{R}^d \rightarrow \mathbb{R}$  be a symmetric function with continuously differentiable partial derivatives. Then  $f$  is Schur-convex if and only if for all  $\mathbf{x} \in \mathbb{R}^d$  and for all  $1 \leq i, j \leq d$ , the following inequality holds:

$$(x_i - x_j) \left( \frac{\partial f}{\partial x_i} - \frac{\partial f}{\partial x_j} \right) \geq 0.$$

The following result is proven in Appendix A-B.

**Theorem III.5** (Schur-Convexity of MAF). *Let  $\bar{\mathbf{G}} = \{\bar{g}_1, \dots, \bar{g}_n\}$  denote a single clipped gradient vector of dimension  $n$ , where each coordinate  $\bar{g}_i$  is obtained by applying  $\ell_2$  clipping to the original gradient followed by independent Laplace noise. Let  $\alpha_{\bar{g}_i}(\lambda)$  denote the moments accountant function for coordinate  $i$ .*

*Then, the total moments accountant function*

$$\alpha_{\bar{\mathbf{G}}}(\lambda) = \sum_{i=1}^n \alpha_{\bar{g}_i}(\lambda) \quad (\text{III.6})$$

*is Schur-convex with respect to the vector of unsigned marginal clipped gradients, i.e., the coordinate-wise magnitudes  $|\bar{g}_1|, \dots, |\bar{g}_n|$ .*

With  $\alpha(\lambda)$  being Schur-convex, we now introduce a majorization set over  $\mathbf{G}$ , the  $\ell_2$  clipped (but not noisy) gradient vector. The following result is proven in Appendix A-C.

**Lemma III.6** (Majorization Set Construction). *Let  $\bar{\mathbf{G}} = \{\bar{g}_1, \dots, \bar{g}_n\}$  denote a single clipped gradient vector of dimension  $n$ , where each coordinate  $\bar{g}_i$  is obtained by applying  $\ell_2$*

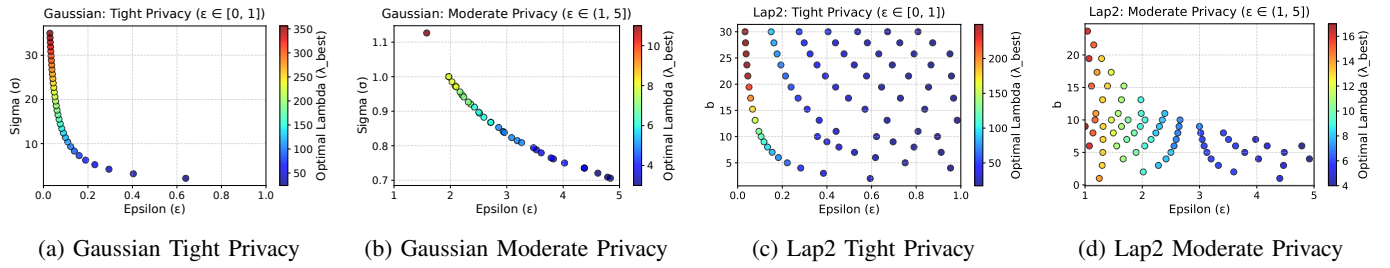


Fig. 3: In Gaussian DP-SGD, the so-called *privacy wall* leads to sharp increases in the noise multiplier under tight privacy ( $\epsilon < 0.5$ ). This arises because the injected noise scales with  $\sigma \cdot C$ , which becomes problematic in settings like pretraining where large  $C$  is needed to preserve gradient signal—resulting in excessive noise. In contrast, LAP<sub>2</sub> supports larger noise or larger clipping norms (see Appendix B-A), due to its heavy tails and efficient high-order moments accounting.

clipping to the original gradient. Then,  $\mathbf{G}$  is weakly majorized by the vector  $x = \{x_1, \dots, x_n\}$  defined by

$$x_i = C \left( \sqrt{i} - \sqrt{i-1} \right), \quad i = 1, \dots, n,$$

where  $C$  is the  $\ell_2$  clipping threshold. That is,  $\mathbf{G} \prec_w x$ .

We now extend the uni-variate moments accountant to the multivariate setting by summing across coordinates, where each coordinate  $i$  uses its corresponding majorization bound  $x_i$ . The following theorem naturally follows from Theorems III.2, III.5, and Lemma III.6.

**Theorem III.7** (Subsampled Multi-variate Laplace Mechanism). *Let  $\mathbf{G} = \{\mathbf{g}_1, \dots, \mathbf{g}_n\}$  be the set of differentially private gradients obtained by applying  $C$ - $\ell_2$  clipping followed by a multi-variate Laplace mechanism with scale  $b$  and sampling probability  $\zeta$ . Define the majorization set  $x = \{x_1, \dots, x_n\}$  by  $x_i = C(\sqrt{i} - \sqrt{i-1})$ ,  $i = 1, \dots, n$ . Then, the total moments accountant satisfies*

$$\alpha_{\mathbf{G}}(\lambda) \leq \sum_{i=1}^n \log \left[ \sum_{\eta=0}^{\lambda+1} \binom{\lambda+1}{\eta} (1-\zeta)^{\lambda+1-\eta} \zeta^\eta F(x_i, \eta) \right], \quad (\text{III.7})$$

where

$$F(x_i, \eta) = \frac{\eta e^{\frac{(\eta-1)x_i}{b}} + (\eta-1)e^{-\frac{\eta x_i}{b}}}{2\eta - 1}. \quad (\text{III.8})$$

#### IV. ANALYSIS AND FRAMEWORK

In this section, we provide a theoretical analysis of LAP<sub>2</sub>, including per-round privacy accounting, utility measured by the signal-to-noise ratio, and insights into parameter selection.

##### A. Privacy Accounting: LAP<sub>2</sub> vs Gaussian

Analyzing Equations II.10 and III.7, the moments accountant functions (MAFs) for the subsampled LAP<sub>2</sub> and Gaussian mechanisms, yields two critical observations:

(1) **Lap<sub>2</sub> mitigates the privacy wall.** Differentially private training is fundamentally constrained by two characteristic limits, termed *two-sided privacy walls*. The **left wall**, which primarily affects the Gaussian mechanism, emerges in the high-privacy regime ( $\epsilon \rightarrow 0$ ) where  $\delta(\epsilon)$  approaches 1. In this regime, increasing the noise scale yields little to no additional privacy gain, indicating the onset of *privacy saturation*. While

both Gaussian and Laplace mechanisms exhibit this saturation behavior, the Gaussian variant suffers more severely due to the rapid rise in its DP failure term  $\delta$ , which can render its guarantees vacuous. The **right wall** arises in the low-privacy regime ( $\epsilon \gg 1$ ), where the effective signal-to-noise ratio (SNR) no longer improves with larger  $\epsilon$ , marking the onset of *utility saturation*. Between these limits lies a narrow *privacy corridor* in which both privacy and accuracy remain meaningful.

Unlike the Gaussian mechanism, LAP<sub>2</sub> demonstrates strong resistance to the left privacy wall, as seen in Figure 3a and 3b and previously noted in [13], [14]. This stability arises from the heavier tails of Laplace noise (Equation III.8), which allow more efficient privacy budget consumption in both high- and low-privacy regimes. Figure 3d and 3d further shows this advantage over different clipping values and their optimal moment orders  $\lambda^*$ , where smaller clipping values (dominant in high-privacy settings) correspond to larger exploitable moments.<sup>3</sup>

Figure 4 summarizes these phenomena for CNN training on MNIST under Gaussian and LAP<sub>2</sub> DP-SGD at subsampling rates  $q \in \{10^{-3}, 10^{-2}, 10^{-1}\}$ . In the **right-wall regime** (top row), the slope  $W_R(\epsilon) = |d \log \sigma / d \log \epsilon|$  deviates from the ideal  $1/\epsilon$  scaling, signaling diminishing utility returns. In the **left-wall regime** (bottom row),  $\delta_g(\epsilon)$  increases faster than  $\delta_{L_2}(\epsilon)$ , and the first  $\epsilon$  satisfying  $\delta_g > 2\delta_{L_2}$  marks the onset of privacy saturation. As  $q$  increases, both walls move inward, narrowing the privacy corridor. Overall, LAP<sub>2</sub> consistently delays both boundaries relative to Gaussian DP-SGD, expanding the stable region of privacy-utility trade-offs.

A practical limitation remains for large-scale models: summing moment-aggregated functions (MAFs) across millions of coordinates, as required by majorization (Equation III.7), inflates the overall privacy bound. Hence, LAP<sub>2</sub> is most effective for small- to medium-scale architectures such as MobileNet and compact ResNet variants (e.g., ResNet-18), where the two walls remain well-separated and its benefits are most pronounced.

(2) **Clipping-aware accounting.** Traditional DP-SGD decouples clipping and noise addition— $\sigma$  governs the privacy guarantee, while  $C$  only scales the added noise. In contrast, our LAP<sub>2</sub>-based accounting (Theorem A-A) integrates  $C$  directly

<sup>3</sup>LAP<sub>2</sub> results are based on a 26K-parameter CNN with  $\delta = 10^{-5}$ .

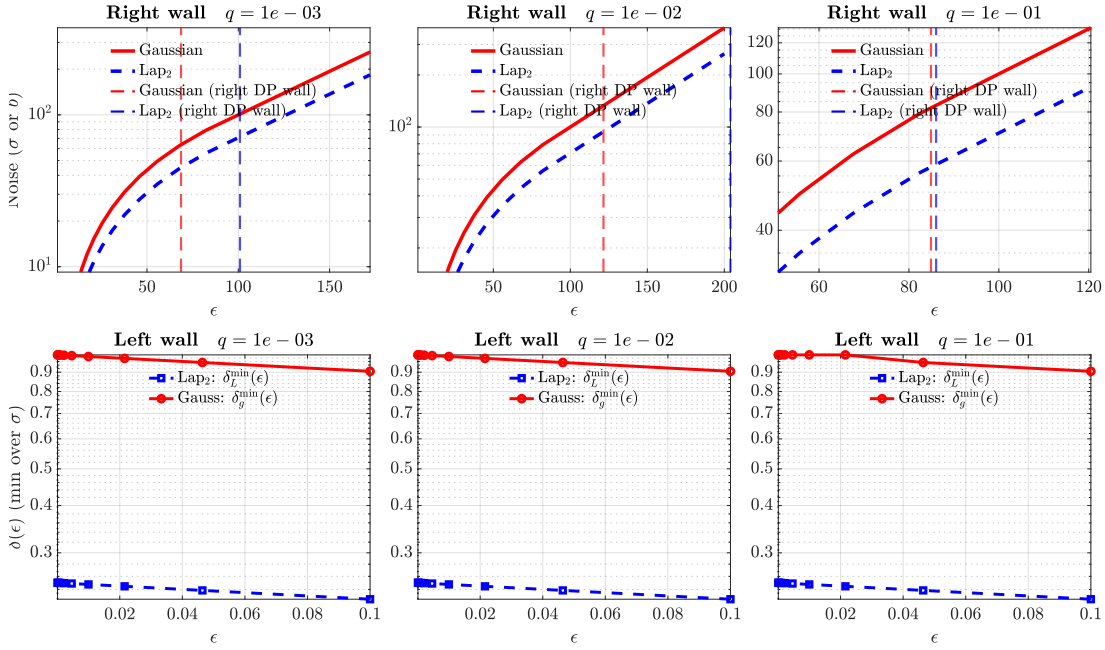


Fig. 4: **Illustration of two-sided privacy walls** (left and right walls) during CNN training on the MNIST dataset under DP-SGD. The *left wall* corresponds to the high-privacy regime, where the noise scale saturates and  $\delta(\epsilon)$  approaches 1, indicating limited further privacy gain. The *right wall* corresponds to the low-privacy regime, where the effective signal-to-noise ratio no longer improves with larger  $\epsilon$ . Together, these walls define the practical operating range (privacy corridor) in which training remains both private and useful.

into the moments accountant, resulting in tighter privacy bounds and more favorable inflection points.

Figure 5 empirically supports this claim: with accountant-adjusted  $b$ , larger  $C$  values yield over 90% accuracy at moderate privacy budgets (e.g.,  $\epsilon = 5$ ). Under tighter budgets (e.g.,  $\epsilon = 1$ ), smaller  $C$  is required, leading to reduced utility. Furthermore, we performed a grid search over the configurations  $(q, C, b)$  to identify the optimal setting for  $\epsilon = 0.5, 1, 2$ , respectively, and  $\delta = 10^{-5}$ . The results of this search are presented in Figure 6, which shows the accuracy of the CNN trained on the MNIST dataset. The optimal configuration (from optimizer) stays within the optimal - yellow region and is highlighted using star mark in the figure.

### B. Optimal Parameter Selection

Let each individual gradient be clipped to norm  $C$  with the sampling rate  $\zeta = B/N$ , batch size  $B$  and dataset size  $N$ . In a single step, the expected signal contribution per example is  $C/B$  with probability  $\zeta$ , and zero otherwise. Over  $T$  steps, the accumulated signal per sample is thus  $\zeta TC/B = TC/N$ , and its squared norm scales as  $T^2 C^2/N^2$ .

In Gaussian DP-SGD, the total noise added per step is  $\sigma C$ , so the noise variance over  $T$  steps is  $TC^2 \sigma^2/B^2$ . This motivates the signal-to-noise ratio (SNR)

$$\eta^2 = \frac{T^2 C^2/N^2}{TC^2 \sigma^2/B^2} = \frac{TC^2}{N^2} \cdot \frac{B^2}{C^2 \sigma^2} = \frac{TB^2}{N^2 \sigma^2} = \frac{T\zeta^2}{\sigma^2}.$$

This is the key driver of utility–privacy tradeoff: as shown in [14], the RDP privacy loss  $\epsilon$  under Gaussian DP-SGD can

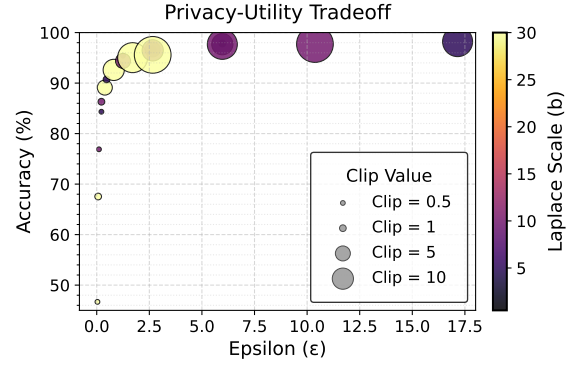


Fig. 5: Accuracy vs. privacy budget  $\epsilon$  for different clipping norms  $C$  using LAP<sub>2</sub> (CNN on MNIST,  $\delta = 10^{-5}$ ). Increasing  $C$  improves utility under moderate  $\epsilon$  due to stronger signal retention, but high  $C$  becomes suboptimal for very tight  $\epsilon$  as noise grows superlinearly.

be approximated as

$$\epsilon_{RDP} \approx \eta^2 + 2\eta\sqrt{\log(1/\delta)}.$$

We refer to  $\eta = \zeta/\sigma$  as the *per-step SNR*, and  $\eta^2 = T\zeta^2/\sigma^2$  as the *total SNR* across  $T$  steps.

**Extension to LAP<sub>2</sub>.** Unlike the Gaussian mechanism, where  $\sigma$  and  $C$  appear as a multiplicative pair in the total noise, the multivariate Laplace mechanism used in LAP<sub>2</sub> introduces noise drawn from a symmetric Laplace distribution with dispersion  $b$ , while gradient sensitivity is controlled by clipping to  $C$ . In this setting, privacy loss depends on the ratio  $\rho = \frac{C}{b}$ ,

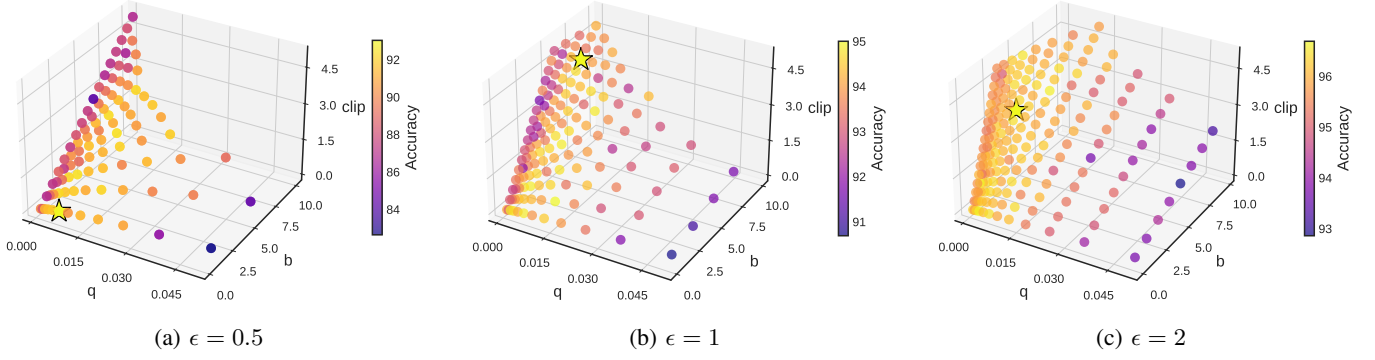


Fig. 6: Accuracy of a CNN trained on MNIST under DP-SGD with  $LAP_2$  for 20 epochs. Configurations  $(q, b, c)$  were selected via grid search for each target privacy budget  $\epsilon \in \{0.5, 1, 2\}$  and  $\delta = 10^{-5}$ , with color indicating the resulting accuracy. The star marks the configuration achieving maximum accuracy for each  $\epsilon$ .

which we refer to as the *privacy-relevant sensitivity-to-noise ratio*. Figure 5 confirms that increasing  $\rho = C/b$  (subject to DP constraints) yields consistent accuracy gains.  $\rho$  also governs the growth of moment terms in the privacy accountant. Specifically, in the small- $\zeta$ , small- $\rho$  regime, the moments accountant satisfies

$$\alpha(\lambda) \approx T\zeta^2\kappa_\lambda\rho^2, \quad \text{where} \quad \kappa_\lambda = \frac{\lambda(\lambda+1)}{2(2\lambda+1)}.$$

Plugging into the MAF $\rightarrow$ DP conversion,

$$\epsilon(\delta) \approx \min_{\lambda>0} \left( \frac{T\zeta^2\kappa_\lambda\rho^2}{\lambda} - \frac{\log \delta}{\lambda} \right),$$

which yields an optimal  $\rho^*$  under privacy target  $\epsilon_{\text{tar}}$  and failure probability  $\delta$ :

$$\rho^* \approx \frac{\epsilon_{\text{tar}}}{2\zeta} \sqrt{\frac{1}{T \log(1/\delta)}}.$$

From this, we obtain a first-order estimate of the optimal noise parameter  $b$  in terms of a chosen clipping norm  $C$ :

$$b^* \approx \frac{2\zeta}{\epsilon_{\text{tar}}} \sqrt{T \log(1/\delta)} C.$$

This formula gives a closed-form initialization for  $(C, b)$ , which can then be refined using exact privacy computation (e.g., Algorithm 1). In practice, we recommend choosing  $C$  based on utility constraints (e.g., a percentile of per-example gradient norms), and computing  $b$  accordingly using the expression above.

### C. The $Lap_2$ Framework

The  $Lap_2$  framework enables practical  $(\epsilon, \delta)$ -DP training under  $l_2$  clipping with Laplace noise. To balance privacy and utility,  $Lap_2$  optimizes the clipping threshold  $C$  under a fixed privacy budget  $(\epsilon, \delta)$ . Unlike in Gaussian DP-SGD where clipping is decoupled from noise, our framework leverages a signal-to-noise ratio (SNR) interpretation where the signal grows with  $C$  and the noise is implicitly governed by  $b$ , the Laplace scale. Specifically, under our  $l_2$ -clipped Laplace mechanism, the per-step SNR is approximated by:  $\eta = \frac{C}{b}$ , and total SNR across  $T$  steps is  $\eta^2 T$ . A higher SNR implies better

utility; hence, we aim to maximize  $\eta$ —equivalently, maximize  $C$  for a fixed  $b$ , subject to satisfying the privacy constraint  $\epsilon(C, b) \leq \epsilon_{\text{target}}$ . This motivates the following optimization problem:

$$\max_{C, b} \frac{C}{b} \quad \text{s.t.} \quad \epsilon(C, b) \leq \epsilon_{\text{target}}, \quad C, b > 0.$$

Due to the non-linear nature of the privacy computation (based on majorization and moments accounting), we perform a grid or binary search to efficiently explore feasible  $(C, b)$  pairs. While the default implementation in Algorithm 1 uses grid search over  $(C, b)$  ranges, a potential enhancement is to replace the inner loop with a binary search over  $b$  for each fixed  $C$ . This accelerates convergence towards the optimal pair  $(C^*, b^*)$  satisfying the privacy constraint.

In practice, we increment  $C$  in ascending order (e.g., logarithmic or linear grid), and for each candidate  $C$ , we search for the smallest  $b$  such that the moments accountant returns  $\epsilon(C, b) \leq \epsilon_{\text{target}}$ . The largest  $C$  satisfying this constraint yields the highest possible SNR. This process is formalized in Algorithm 1, and the resulting  $(C^*, b^*)$  pair is passed to the DP-SGD loop in Algorithm 2 in Appendix.

## V. EXPERIMENTS

In this section, we evaluate the performance of our  $LAP_2$  mechanism in terms of privacy, accuracy, and efficiency on computer vision (CV) and natural language processing (NLP) tasks. First, we compare the utility performance with two baselines: the standard DP-SGD using Gaussian noise, and the classical Laplace mechanism with  $l_1$ -norm clipping.

### A. Experimental Settings

**Computer Vision Datasets and Tasks.** Image classification experiments were performed using three standard datasets: CIFAR-10, MNIST, and Fashion-MNIST. The CIFAR-10 dataset contains 60,000  $32 \times 32$  color images across 10 classes (6,000 per class), divided into 50,000 training and 10,000 test images. The MNIST dataset consists of 70,000  $28 \times 28$  grayscale images of handwritten digits (0–9), with 60,000 for training and 10,000 for testing. Similarly, the Fashion-MNIST

TABLE I: Hyperparameter settings for different CV datasets and models.

Dataset	Model	Sampling Rate	Clipping Threshold	$\delta$	Learning Rate	Label Smoothing	Weight Decay	Training Steps
MNIST	CNN	0.0043	1	$1 \times 10^{-5}$	$1 \times 10^{-3}$	0.15	$1 \times 10^{-4}$	5860
Fashion-MNIST	CNN	0.0043	1	$1 \times 10^{-5}$	$1 \times 10^{-3}$	0.15	$1 \times 10^{-4}$	5860
CIFAR-10	ViT	0.01668	1	$1 \times 10^{-5}$	$1 \times 10^{-3}$	0	$1 \times 10^{-4}$	900

**Algorithm 1** Lap<sub>2</sub> Parameter  $b$  Optimizer (via Binary Search)

**Input:** rounds  $T$ , sampling rate  $\zeta$ , privacy target  $(\epsilon, \delta)$ ,  
max values  $C_{\max}, b_{\max}$ ; resolution  $\Delta_C$ , binary tolerance  $\tau$   
**Output:** optimal  $(C^*, b^*)$  maximizing  $C$  under  $(\epsilon, \delta)$   
 $C^* \leftarrow 0, b^* \leftarrow \text{None}$   
**for**  $C$  in  $[C_{\min}, C_{\max}]$  **step**  $\Delta_C$  **do**  
     $b_{\text{low}} \leftarrow b_{\min}, b_{\text{high}} \leftarrow b_{\max}$   
    **while**  $b_{\text{high}} - b_{\text{low}} > \tau$  **do**  
         $b \leftarrow (b_{\text{low}} + b_{\text{high}})/2$   
        Define majorization set:  $x_i = C \cdot (\sqrt{i} - \sqrt{i-1})$  for  $i = 1$  to  $n$   
        Initialize total accountant  $\alpha \leftarrow 0$   
        **for**  $t = 1$  to  $T$  **do**  
            Compute  $F(x_i, \eta)$  and moments  $\alpha_t$  (see Equation III.7)  
             $\alpha \leftarrow \alpha + \alpha_t$   
        **end for**  
        Compute  $\epsilon_C(b)$  from moment accountant  
        **if**  $\epsilon_C(b) \leq \epsilon$  **then**  
             $b_{\text{high}} \leftarrow b$   
        **else**  
             $b_{\text{low}} \leftarrow b$   
    **end while**  
    **if**  $b_{\text{high}} < b_{\max}$  **and**  $C > C^*$  **then**  
         $(C^*, b^*) \leftarrow (C, b_{\text{high}})$   
**end for**  
**return**  $(C^*, b^*)$

dataset includes 70,000  $28 \times 28$  grayscale images of 10 clothing categories. The full dataset was used for evaluation.

**CV Models.** Testing with MNIST and Fashion MNIST was done on a small 4-layer CNN model as described in the [Tensorflow privacy tutorial](#) for CV tasks. Testing with CIFAR-10 was done with a ViT [36] model with a patch size of 16, as sourced from the [TIMM Repository](#). The images were scaled to the expected input size of  $224 \times 224$  pixels for the ViT model. No other augmentations were applied to the images.

**Natural Language Processing Datasets and Tasks.** We first evaluate the LAP<sub>2</sub> on the sentiment analysis tasks from the GLUE benchmark [4]. Specifically, following [2], we fully fine-tune the RoBERTa-base model on SST-2 and QNLI datasets [4]. These datasets are widely used to evaluate private training. SST-2 has more than 60k samples in the training set and 1,821 samples in the test set; QNLI has more than 100k samples in the training set and 5,463 samples in test, including two classes. We also evaluate the table-to-text generation task’s performance that generates the table entries’ descriptions. We fine-tune the DistilGPT2 model [2] with the E2E dataset [3].

**Experimental Platform.** Experiments were conducted on three systems optimized for specific tasks: (1) a high-end workstation with an AMD Ryzen Threadripper PRO 5975WX (32 cores, 64 threads), 500 GB RAM, and  $3 \times$  NVIDIA Quadro RTX A6000 (48 GB) GPUs for NLP tasks; (2) a virtualized

server with up to 192 CPU cores (Intel Xeon Platinum and AMD EPYC), 1 TB RAM, used primarily for ViT training; and (3) a consumer-grade system with an AMD Ryzen 7 8700F (8 cores, 16 threads), 32 GB RAM, and an NVIDIA RTX 3060 (12 GB VRAM) for CNN and ViT experiments on MNIST, Fashion-MNIST, and CIFAR-10.

**B. Utility Evaluation**

TABLE II: Comparison of Gaussian, Laplace ( $\ell_1$  norm), and LAP<sub>2</sub> ( $\ell_2$  norm) mechanisms across different  $\epsilon$ .

$\epsilon$	Gaussian (%)	Laplace (%)	LAP <sub>2</sub> (%)
<b>CNN on MNIST</b>			
3.42	97.27	51.82	96.82
2.53	97.19	46.67	96.90
1.68	97.42	28.82	95.39
0.88	96.08	16.44	93.29
0.13	87.44	10.40	78.96
<b>CNN on FMNIST</b>			
3.42	83.67	55.05	82.60
2.53	83.09	43.85	81.45
1.68	82.34	43.94	81.45
0.88	80.34	28.22	77.03
0.13	72.58	14.74	70.03
<b>ViT on CIFAR-10 (Fine-tuning)</b>			
0.75	97.17	53.58	98.11
0.5	96.90	47.04	98.18

**Utility of CV Tasks.** To demonstrate the efficacy of the proposed LAP<sub>2</sub> framework, we first discuss results of classification on the CV datasets (MNIST and Fashion-MNIST datasets) using a small 4-layer CNN, shown in Table II. The privacy budget is in the range 0.1 to 3.5. Other training details is shown in the Table I. Specifically, we compare the test accuracy achieved using the Gaussian mechanism, the Laplace mechanism with the  $\ell_1$  norm, and the LAP<sub>2</sub> mechanism. The first key trend observed is that test accuracy increases with larger values of  $\epsilon$ , reflecting the fundamental trade-off between privacy and utility: a higher  $\epsilon$  relaxes the privacy constraint, allowing less noise to be added and thereby improving model performance. The Gaussian mechanism performs well across the board, achieving over 96% accuracy on MNIST when  $\epsilon \geq 0.88$ , and over 80% on FMNIST. However, the Laplace mechanism with the  $\ell_1$  norm consistently yields poor results. For instance, on MNIST with  $\epsilon = 0.88$ , it only achieves 16.44% accuracy far below the Gaussian (96.08%) and LAP<sub>2</sub> (93.29%). On FMNIST, the performance gap is similarly large. This degradation is primarily due to the substantially larger  $\ell_1$  norm of the gradient vector compared to its  $\ell_2$  counterpart, which results in gradient loss during clipping during training. In contrast, the LAP<sub>2</sub> mechanism consistently matches or closely follows the performance of the Gaussian mechanism

across all  $\epsilon$  values. On MNIST, its accuracy remains above 93% for  $\epsilon \geq 0.88$ , and still reaches 78.96% at the extremely strict privacy level of  $\epsilon = 0.13$ , a 68.6 percentage point gain over Laplace with the  $\ell_1$  norm.

Furthermore, we fine-tune the ViT model on the CIFAR-10 dataset instead of training from scratch. The last section in Table II presents the fine-tuning results of the ViT model on the CIFAR-10 dataset under different noise mechanisms. For the privacy bound  $\epsilon = 0.75$ , the Gaussian and Laplace ( $\ell_1$ -clipping) mechanisms achieve accuracies of 97.17% and 53.58%, respectively, while LAP<sub>2</sub> attains a superior accuracy of 98.11%. Similarly, for  $\epsilon = 0.5$ , the Gaussian and Laplace ( $\ell_1$ ) methods yield 96.90% and 47.04%, whereas LAP<sub>2</sub> achieves 98.18%. These results demonstrate that the proposed LAP<sub>2</sub> mechanism consistently outperforms both Gaussian and Laplace ( $\ell_1$ ) approaches across different privacy budgets, highlighting its robustness and effectiveness for fine-tuning ViT models under differential privacy guarantees.

TABLE III: Comparison of Gaussian, Laplace ( $\ell_1$  norm), and LAP<sub>2</sub> ( $\ell_2$  norm) mechanisms across different privacy levels ( $\epsilon$ ) for RoBERTa-base on SST-2 and QNLI.

$\epsilon$	Gaussian (%)	Laplace (%)	LAP <sub>2</sub> (%)
<b>RoBERTa-base on SST-2</b>			
3.7382	90.31	50.34	90.11
1.1584	89.65	50.21	83.32
0.9108	89.23	50.15	89.14
0.5384	87.16	48.97	87.88
<b>RoBERTa-base on QNLI</b>			
3.6452	83.26	50.76	83.73
1.1365	82.61	50.49	82.52
0.9345	82.17	50.18	82.87
0.5168	80.41	49.97	60.87

**Utility of Sentiment Analysis (NLP).** We conducted fine-tuning experiments for sentiment analysis using the SST-2 and QNLI datasets with the RoBERTa-base model. Table III presents the model accuracy under various privacy levels ( $\epsilon \in 0.5, 0.9, 1.1, 3.7$ ), comparing our proposed LAP<sub>2</sub> mechanism with the Gaussian mechanism and the standard Laplace mechanism using the  $\ell_1$  norm clipping. As observed, the Laplace mechanism with the  $\ell_1$  norm consistently yields accuracy around 50% across all  $\epsilon$  values on both datasets. This is close to the baseline performance of the pretrained model without fine-tuning, suggesting that the injected noise is so severe that the model fails to learn from the downstream task, rendering fine-tuning ineffective.

In contrast, our proposed LAP<sub>2</sub> mechanism consistently matches or outperforms the Gaussian mechanism across all  $\epsilon$  values and both datasets (similar to our findings in the computer vision tasks). For the SST-2 dataset, LAP<sub>2</sub> achieves similar result as Gaussian when  $\epsilon$  is large ( $\epsilon = 3.7$ ). For the QNLI dataset, the trend is even more pronounced: the gap grows from roughly 0.5% at  $\epsilon = 3.6$ . These results clearly demonstrate that LAP<sub>2</sub> maintains strong utility under strong privacy guarantees with Laplace noise, especially in the context of large pre-trained language models.

**Performance on Generation Task (NLP).** Table IV presents the results from fine-tuning the DistilGPT-2 model with the

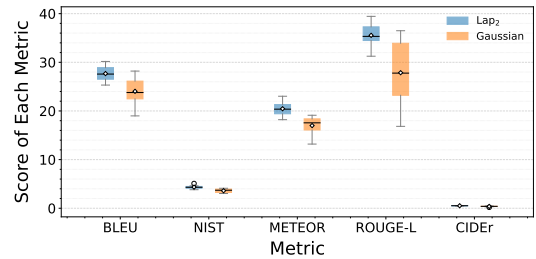


Fig. 7: Gaussian and LAP<sub>2</sub> mechanisms on the DistilGPT-2 model and E2E dataset for the generation task (batch size  $B = 80$ , clipping value  $C = 2$ , and  $\epsilon = 1$ ).

TABLE IV: Metrics of Gaussian and LAP<sub>2</sub> mechanisms applied to the DistilGPT-2 model on the E2E dataset for the generation task.

Metric	Noise Type	$\epsilon = 1.2$	$\epsilon = 1$	$\epsilon = 0.4$
BLEU	Gaussian	23.39	22.83	16.16
	LAP <sub>2</sub>	<b>27.99</b>	<b>27.34</b>	<b>26.90</b>
NIST	Gaussian	3.9474	3.5342	2.7025
	LAP <sub>2</sub>	<b>4.4001</b>	<b>4.3100</b>	<b>4.1200</b>
METEOR	Gaussian	16.84	16.73	15.20
	LAP <sub>2</sub>	<b>20.50</b>	<b>20.20</b>	<b>19.80</b>
ROUGE-L	Gaussian	33.49	32.88	32.50
	LAP <sub>2</sub>	<b>36.85</b>	<b>36.62</b>	<b>34.20</b>
CIDEr	Gaussian	0.3385	0.3232	0.2586
	LAP <sub>2</sub>	<b>0.5301</b>	<b>0.5152</b>	<b>0.4650</b>

E2E dataset, using five different metrics by following [2]; Besides, we present the boxplot of Gaussian and LAP<sub>2</sub> mechanisms at  $\epsilon = 1$  in Figure 7. Specifically, BLEU measures the  $n$ -gram precision between the generated and reference sentences; NIST is a variant of BLEU that weights informative  $n$ -grams more heavily, emphasizing rare but meaningful word sequences; METEOR incorporates both precision and recall through word alignments and synonym matching; ROUGE-L computes the longest common subsequence between the generated and reference texts, reflecting overall sentence-level fluency and content coverage; CIDEr measures the cosine similarity between TF-IDF-weighted  $n$ -gram vectors of the candidate and reference sentences. For each metric, larger values mean more accurately generated texts. For every metric evaluated and for every privacy value used, the model trained using our proposed LAP<sub>2</sub> mechanism outperformed the model trained with the Gaussian mechanism. It is worth noting that the improvement can be up to around 50% on some metrics (e.g., CIDEr). We observe that the LAP<sub>2</sub> mechanism yields results that are more closely aligned with the non-private results. Recall that the performance of the Gaussian and LAP<sub>2</sub> mechanisms may vary slightly due to randomness. However, the overall comparative trend remains consistent across mechanisms (see both Table IV and Figure 7), supporting our main conclusion that our approach effectively bridges the performance gap of the Laplace mechanism in AI training,

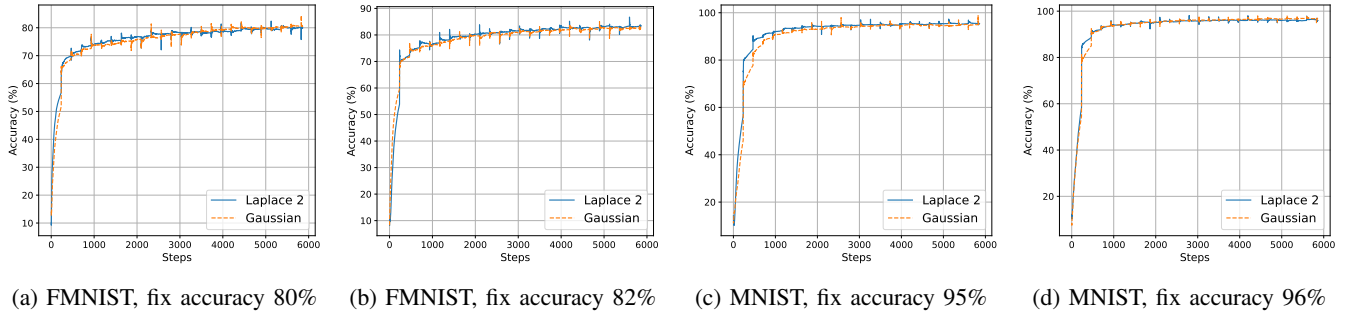


Fig. 8: Runtime comparison on CNN model with MNIST or FMNIST datasets.

particularly for large models, achieving results comparable to Gaussian-based DP-SGD.

### C. Runtime Evaluation

To further evaluate the utility and efficiency of our proposed  $LAP_2$  mechanism, we compare its **convergence time** with the standard Gaussian mechanism under the same accuracy. Figure 8 presents the test accuracy versus training steps on a CNN model under fixed accuracy targets.

In FMNIST with a target accuracy of 80% (Figure 8a) and 82% (Figure 8b),  $LAP_2$  achieves the desired accuracy with similar steps as Gaussian mechanism (within  $\pm 2\%$  difference in training steps across runs). For the MNIST dataset with target accuracies of 95% (Figure 8c), the  $LAP_2$  mechanism shows that the convergence time is obviously faster convergence. Thus, across all tasks, we observe that  $LAP_2$  achieves comparable convergence time to Gaussian, requiring a similar number of training steps to reach the same accuracy. While minor differences exist (e.g., in MNIST with 95% accuracy,  $LAP_2$  appears slightly faster), overall the two mechanisms behave similarly in terms of convergence speed. These results indicate that our  $LAP_2$  mechanism **maintains model trainability** and does not introduce convergence delays compared to the standard Gaussian approach, even under strict privacy constraints.

### D. Discussion

**Empirical Insights.** The empirical evaluation demonstrates that  $LAP_2$  provides a *practical, stable, and theoretically grounded* alternative to Gaussian DP-SGD. Across both vision and language benchmarks (MNIST, CIFAR-10, GLUE, and DistilGPT-2),  $LAP_2$  achieves *comparable accuracy and convergence stability* under equivalent privacy budgets, with particularly strong performance in high-privacy regimes ( $\epsilon \leq 1$ ). Figures 4 shows that  $LAP_2$  effectively *delays both privacy walls*, maintaining usable signal-to-noise ratio (SNR) and non-vacuous  $\delta(\epsilon)$  bounds over a broader privacy corridor. On larger models such as RoBERTa-base and DistilGPT-2,  $LAP_2$  remains robust across evaluation metrics, while runtime analysis (Figure 8) confirms that these gains are achieved with *no additional computational overhead*. Together, these indicate that  $LAP_2$  preserves both training utility and efficiency.

**Adaptive Clipping and Integration with  $LAP_2$ .** Recent advances in Gaussian DP-SGD have introduced *adaptive clip-*

*ping strategies* that dynamically adjust the clipping threshold  $C_t$  to balance gradient distortion and noise injection, replacing the traditional fixed clipping constant. Three representative approaches are particularly relevant:

- **Galli et al. [37]** propose *Online Sensitivity Optimization*, which learns the optimal  $C_t$  online through privatized gradient-norm feedback, thereby minimizing privacy-aware training loss.
- **Zhang et al. [38]** introduce *DiceSGD*, an *error-feedback* mechanism that corrects clipping-induced bias, enabling smaller and more problem-independent  $C_t$  without compromising convergence.
- **Chen et al. [39]** extend these ideas with *per-layer adaptive clipping*, assigning a separate  $C_{t,\ell}$  to each layer based on privatized gradient statistics, thereby balancing layer-wise sensitivity.

Integrating such strategies into  $LAP_2$  is straightforward. Our FAST  $LAP_2$  accountant depends solely on the ratio  $r_t = C_t/b_t$ , which can vary across iterations without violating composition guarantees. Hence, adaptive  $C_t$  updates modify only the *sensitivity term*, leaving the majorization-based accounting framework intact. Empirically, this adaptation is expected to shift the  $\epsilon$ -accuracy curve upward, reducing clipping bias while maintaining privacy, with the largest benefits observed in high-privacy regimes ( $\epsilon \leq 1$ ). Preliminary experiments on MNIST show that integrating adaptive clipping improves accuracy by 0.4–0.8% and reduces variance across runs. Extending experiments to larger architectures such as ViT and DistilGPT-2 constitutes a promising future work.

## VI. RELATED WORK

The majority of research on DP-SGD has focused on the Gaussian mechanism [10] due to its smooth noise distribution with gradient updates and facilitates privacy accounting using the moments accountant framework [10].

**Recent Development in DP-SGD.** Several studies have since optimized DP-SGD along different dimensions, as summarized in Table V. These works can be broadly categorized into:

- **Memory-efficient methods:** e.g., GHOST [40], PEFT [2], and Per-layer Clip [41] reduce memory overhead by modifying gradient computation or clipping;
- **Time-efficient methods:** e.g., DP-SGD-JL [42], Mixed Ghost [43], and DP-BiTfIT [44] focus on reducing computational cost while maintaining DP guarantees;

- Accuracy-enhancing methods: e.g., DPSUR [45], DP-Forward [46], and ViP [47] aim to improve utility by refining gradient updates or leveraging structured noise.

While most of these methods focus on the Gaussian mechanism, Table V highlights that no existing DP-SGD variants have applied Laplace noise for large-scale NLP or vision tasks. Beyond efficiency improvements, prior work has also refined privacy analysis in DP-SGD. Wang et al. [48] examined subsampling effects on privacy guarantees, while Gopi et al. [12] developed a numerical approach to compute privacy loss precisely. These accounting refinements could be leveraged alongside Lap<sub>2</sub> to achieve tighter privacy budgets.

Prior work has improved DP-SGD through refined noise design and tighter privacy-loss analysis. Our recent work [49] optimizes the privacy-loss random variable (PLRV) via randomized noise-scale selection to enhance the privacy-utility trade-off. In contrast, this work enables  $\ell_2$ -clipped Laplace DP-SGD using a majorization-based multivariate moments accountant, addressing the limitations of standard Laplace training. Also, Liu et al. [50] derive concentration bounds for product-measure PLRVs via a magnitude-direction decomposition, further highlighting the value of PLRV-centric analysis for tight privacy accounting in high-dimensional settings.

**DP-SGD with Laplace Mechanism.** The Laplace mechanism was historically considered optimal in many pure  $\epsilon$ -DP settings due to its strong theoretical guarantees and minimal error in certain regimes [9], [51]. Although Gaussian noise later became standard in DP-SGD because of its compatibility with moments accountants, Laplace noise can outperform Gaussian under strong privacy requirements (e.g.,  $\epsilon \rightarrow 0^+$ ) [51]. Privacy loss distribution (PLD)-based accounting further enables tight  $(\epsilon, \delta)$ -DP guarantees for Laplace, Gaussian, and related mechanisms under subsampling [52].

TABLE V: Representative DP methods.  $\perp$ : orthogonal work. L: NLP tasks (language model), V: computer vision tasks.

Existing Methods	Noise	System Focus	Utility Focus	Tasks
GHOST [40]	Gaussian	Memory $\perp$	–	L
DP-SGD-JL [42]	Gaussian	Time/Mem $\perp$	–	L
Mixed Ghost [43]	Gaussian	Time/Mem $\perp$	–	V
PEFT [2]	Gaussian	Memory $\perp$	–	L
Book-Keeping [53]	Gaussian	Time/Mem $\perp$	–	L
Per-layer Clip [41]	Gaussian	Memory $\perp$	–	V, L
DP-BITFiT [44]	Gaussian	Time/Mem $\perp$	–	V, L
DPSUR [45]	Gaussian	Time Deduct $\perp$	Acc (Vision) $\perp$	V
DP-Forward [46]	Matrix Gau.	–	Acc $\perp$	L
ViP [47]	Gaussian	–	Acc (ViT) $\perp$	V
AdaMix [54]	Gaussian	–	Acc $\perp$	V
Multi-Clip [55]	Gaussian	–	Video Acc $\perp$	V
<b>Lap<sub>2</sub> (Ours)</b>	Laplace	Time/Mem	Boost Acc	V, L

Despite these advantages, Laplace DP-SGD has seen limited adoption, mainly due to the instability introduced by  $\ell_1$ -norm gradient clipping required for Laplace sensitivity control, which often harms training utility. Prior works [52], [56], [57] studied the privacy behavior of Laplace subsampled

mechanisms via PLRV-based analyses (e.g., saddle-point approximations, asymptotic bounds, and Edgeworth corrections), but largely focused on  $(\epsilon, \delta)$  characterization rather than empirical utility evaluation. Alternative directions such as DP-signSGD [58], [59] and Laplace-based Bayesian learning [60] adopt different training paradigms and are orthogonal to standard DP-SGD. In contrast, our work introduces Lap<sub>2</sub>, enabling stable DP-SGD with Laplace noise while mitigating the instability caused by  $\ell_1$ -norm clipping.

**Other Improvements on DP-SGD.** Papernot et al. [61] explored modifications to neural network activations that mitigate some of the utility loss incurred by DP noise while still maintaining privacy guarantees.

[62] combines careful hyperparameter tuning with several techniques to normalize the gradients and reduce their variance to ensure signal propagation and improve the convergence rate of DP-SGD on large models.

DP-Adam[63], a similar deep learning training algorithm to DP-SGD, adjusts the learning rate for each parameter individually based on the first and second moments of the gradients to better maintain the expectations of the Adam optimizer. [64] proposes the privacy loss distribution (PLD) based accounting, which allows for tighter  $(\epsilon, \delta)$ -DP guarantees for many popular mechanisms compared to other known methods. This work supports the poisson sub-sampling for additive noises such as Laplace, Gaussian Discrete Laplace, and Discrete Gaussian.

Moreover, there is work [11] to provide tighter conversion between the tracked privacy loss of multiple iterations to the traditional  $(\epsilon, \delta)$ -differential privacy guarantee than [65].

## VII. CONCLUSION

In this work, we proposed LAP<sub>2</sub>, a new framework that resolves a key limitation of traditional Laplace DP-SGD—its dependence on  $\ell_1$  norm clipping—by enabling  $\ell_2$ -clipped Laplace mechanisms with strong privacy guarantees. Leveraging majorization theory and Schur-convexity, LAP<sub>2</sub> constructs a data-independent multivariate moment accountant that scales gracefully with model dimensionality, supports tight privacy analysis, and permits significantly higher clipping norms than Gaussian DP-SGD under equivalent privacy budgets. Our empirical results demonstrate that LAP<sub>2</sub> achieves comparable accuracy to Gaussian DP-SGD. Despite these benefits, we observe that in some computer vision tasks, LAP<sub>2</sub> can still struggle to match the performance of Gaussian DP-SGD, suggesting future directions for improved noise shaping or task-specific calibration. Overall, LAP<sub>2</sub> offers a scalable, efficient, and theoretically grounded alternative for private training of large-scale models, bridging the gap between Laplace mechanisms and modern deep learning.

## ACKNOWLEDGMENTS

We sincerely thank the anonymous reviewers for their constructive comments. This work is partially supported by the National Science Foundation under Grants No. CNS-2302689, CNS-2308730, CNS-2319277, CNS-2432533, ITE-2452747, and ITE-2452749, as well as by a Cisco Research Award.

## REFERENCES

- [1] Yinhan Liu, Myle Ott, Naman Goyal, Jingfei Du, Mandar Joshi, Danqi Chen, Omer Levy, Mike Lewis, Luke Zettlemoyer, and Veselin Stoyanov. Roberta: A robustly optimized bert pretraining approach. *arXiv preprint arXiv:1907.11692*, 2019.
- [2] Da Yu, Saurabh Naik, Arturs Backurs, Sivakanth Gopi, Huseyin A Inan, Gautam Kamath, Janardhan Kulkarni, Yin Tat Lee, Andre Manoel, Lukas Wutschitz, et al. Differentially private fine-tuning of language models. In *International Conference on Learning Representations*, 2021.
- [3] Jekaterina Novikova, Ondřej Dušek, and Verena Rieser. The E2E dataset: New challenges for end-to-end generation. pages 201–206, 2017.
- [4] Alex Wang, Amanpreet Singh, Julian Michael, Felix Hill, Omer Levy, and Samuel R. Bowman. GLUE: A multi-task benchmark and analysis platform for natural language understanding. In *ICLR*, 2019.
- [5] Ahmed Salem, Apratim Bhattacharya, Michael Backes, Mario Fritz, and Yang Zhang. Updates-Leak: Data set inference and reconstruction attacks in online learning. In *USENIX Security*, pages 1291–1308, 2020.
- [6] Jonas Geiping, Hartmut Bauermeister, Hannah Dröge, and Michael Moeller. Inverting gradients - how easy is it to break privacy in federated learning? *NeurIPS*, 2020.
- [7] Gege Qi, YueFeng Chen, Xiaofeng Mao, Binyuan Hui, Xiaodan Li, Rong Zhang, and Hui Xue. Model inversion attack via dynamic memory learning. In *MM*, 2023.
- [8] Nicholas Carlini, Chang Liu, Úlfar Erlingsson, Jeremy Kos, and Dawn Song. The secret sharer: Evaluating and testing unintended memorization in neural networks. In *USENIX Security*, 2019.
- [9] Cynthia Dwork. Differential privacy. In *International colloquium on automata, languages, and programming*, pages 1–12. Springer, 2006.
- [10] Martin Abadi, Andy Chu, Ian Goodfellow, H Brendan McMahan, Ilya Mironov, Kunal Talwar, and Li Zhang. Deep learning with differential privacy. In *Proceedings of the 2016 ACM SIGSAC conference on computer and communications security*, pages 308–318, 2016.
- [11] Borja Balle and Yu-Xiang Wang. Improving the Gaussian mechanism for differential privacy: Analytical calibration and optimal denoising. In *International Conference on Machine Learning*, pages 394–403. PMLR, 2018.
- [12] Sivakanth Gopi, Yin Tat Lee, and Lukas Wutschitz. Numerical composition of differential privacy. *NeurIPS*, 34:11631–11642, 2021.
- [13] Ilya Mironov, Kunal Talwar, and Li Zhang. Rényi differential privacy of the sampled Gaussian mechanism. *arXiv preprint arXiv:1908.10530*, 2019.
- [14] Tom Sander, Pierre Stock, and Alexandre Sablayrolles. Tan without a burn: scaling laws of dp-sgd. In *Proceedings of the 40th International Conference on Machine Learning*, ICML’23. JMLR.org, 2023.
- [15] Naoise Holohan, Spiros Antonatos, Stefano Braghin, and Pól Mac Aonghusa. The bounded laplace mechanism in differential privacy. *arXiv preprint arXiv:1808.10410*, 2018.
- [16] Quan Geng and Pramod Viswanath. The optimal noise-adding mechanism in differential privacy. *IEEE Transactions on Information Theory*, 62(2):925–951, 2015.
- [17] Gokularam Muthukrishnan and Sheetal Kalyani. Differential privacy with higher utility by exploiting coordinate-wise disparity: Laplace mechanism can beat gaussian in high dimensions. *IEEE Transactions on Information Forensics and Security*, 2025.
- [18] Albert W Marshall, Ingram Olkin, and Barry C Arnold. Inequalities: theory of majorization and its applications. 1979.
- [19] Cynthia Dwork, Frank McSherry, Kobbi Nissim, and Adam Smith. Calibrating noise to sensitivity in private data analysis. In *Theory of Cryptography: Third Theory of Cryptography Conference, TCC 2006, New York, NY, USA, March 4-7, 2006. Proceedings 3*, pages 265–284. Springer, 2006.
- [20] Cynthia Dwork, Krishnaram Kenthapadi, Frank McSherry, Ilya Mironov, and Moni Naor. Our data, ourselves: Privacy via distributed noise generation. In *Advances in Cryptology—EUROCRYPT*, pages 486–503, 2006.
- [21] Cynthia Dwork, Frank McSherry, Kobbi Nissim, and Adam Smith. Calibrating noise to sensitivity in private data analysis. In *Proceedings of the Third Conference on Theory of Cryptography (TCC)*, pages 265–284, 2006.
- [22] Cynthia Dwork. Differential privacy. In *Automata, Languages and Programming, 33rd International Colloquium, ICALP 2006, Venice, Italy, July 10-14, 2006, Proceedings, Part II*, pages 1–12, 2006.
- [23] Cynthia Dwork, Krishnaram Kenthapadi, Frank McSherry, Ilya Mironov, and Moni Naor. Our data, ourselves: Privacy via distributed noise generation. In *Advances in Cryptology—EUROCRYPT 2006: 24th Annual International Conference on the Theory and Applications of Cryptographic Techniques, St. Petersburg, Russia, May 28-June 1, 2006. Proceedings 25*, pages 486–503. Springer, 2006.
- [24] Adrian M. Walker. Probability theory and mathematical statistics. by marek fiz. pp. xvi, 677. 115s. 1963. (john wiley and sons: New york, london). *The Mathematical Gazette*, 49:109 – 112, 1965.
- [25] Cynthia Dwork, Moni Naor, Toniann Pitassi, and Guy N. Rothblum. Differential privacy under continual observation. In *Proceedings of the 42nd ACM symposium on Theory of computing*, STOC ’10, pages 715–724, New York, NY, USA, 2010. ACM.
- [26] Cynthia Dwork, Guy N Rothblum, and Salil Vadhan. Boosting and differential privacy. In *2010 IEEE 51st Annual Symposium on Foundations of Computer Science*, pages 51–60. IEEE, 2010.
- [27] Peter Kairouz, Sewoong Oh, and Pramod Viswanath. The composition theorem for differential privacy. *IEEE Information Theory*, 63(6):4037–4049, 2017.
- [28] Peter Kairouz, Sewoong Oh, and Pramod Viswanath. The composition theorem for differential privacy. In *International conference on Machine Learning*, pages 1376–1385. PMLR, 2015.
- [29] Mark Bun, Cynthia Dwork, Guy N. Rothblum, and Thomas Steinke. Composable and versatile privacy via truncated CDP. In *Proceedings of the 50th Annual ACM SIGACT Symposium on Theory of Computing (STOC)*, pages 74–86, 2018.
- [30] Borja Balle, Gilles Barthe, Marco Gaboardi, Justin Hsu, and Tetsuya Sato. Hypothesis testing interpretations and renyi differential privacy. In Silvia Chiappa and Roberto Calandra, editors, *Proceedings of the Twenty Third International Conference on Artificial Intelligence and Statistics*, volume 108 of *Proceedings of Machine Learning Research*, pages 2496–2506. PMLR, 26–28 Aug 2020.
- [31] David M. Sommer, Esfandiar Mohammadi, and Sebastian Meiser. Privacy loss classes: The central limit theorem in differential privacy. *Proceedings on Privacy Enhancing Technologies*, 2019:245 – 269, 2019.
- [32] Depeng Xu, Wei Du, and Xintao Wu. Removing disparate impact on model accuracy in differentially private stochastic gradient descent. In *Proceedings of the 27th ACM SIGKDD Conference on Knowledge Discovery & Data Mining, KDD ’21*, page 1924–1932, New York, NY, USA, 2021. Association for Computing Machinery.
- [33] J. Michael Steele. *The Cauchy-Schwarz Master Class: An Introduction to the Art of Mathematical Inequalities*. Cambridge University Press, 2004.
- [34] Michel Talagrand. Majorizing measures: The generic chaining. *The Annals of Probability*, 24(3):1049–1103, 1996.
- [35] Josip E Peajcariac and Yung Liang Tong. *Convex functions, partial orderings, and statistical applications*. Academic Press, 1992.
- [36] Alexey Dosovitskiy, Lucas Beyer, Alexander Kolesnikov, Dirk Weissenborn, Xiaohua Zhai, Thomas Unterthiner, Mostafa Dehghani, Matthias Minderer, Georg Heigold, Sylvain Gelly, Jakob Uszkoreit, and Neil Houlsby. An image is worth 16x16 words: Transformers for image recognition at scale, 2021.
- [37] Filippo Galli, Catuscia Palamidessi, and Tommaso Cucinotta. Online sensitivity optimization in differentially private learning. In *Proceedings of the AAAI Conference on Artificial Intelligence*, volume 38, pages 12109–12117, 2024.
- [38] Xinwei Zhang, Zhiqi Bu, Zhiwei Steven Wu, and Mingyi Hong. Differentially private sgd without clipping bias: An error-feedback approach. *ArXiv*, abs/2311.14632, 2023.
- [39] Haichao Sha, Yang Cao, Yong Liu, Yuncheng Wu, Ruixuan Liu, and Hong Chen. Clip body and tail separately: High probability guarantees for dpsgd with heavy tails. *arXiv preprint arXiv:2405.17529*, 2024.
- [40] Xuechen Li, Florian Tramer, Percy Liang, and Tatsunori Hashimoto. Large language models can be strong differentially private learners. In *International Conference on Learning Representations*, 2022.
- [41] Jiyan He, Xuechen Li, Da Yu, Huishuai Zhang, Janardhan Kulkarni, Yin Tat Lee, Arturs Backurs, Nenghai Yu, and Jiang Bian. Exploring the limits of differentially private deep learning with group-wise clipping. *arXiv preprint arXiv:2212.01539*, 2022.
- [42] Zhiqi Bu, Sivakanth Gopi, Janardhan Kulkarni, Yin Tat Lee, Hanwen Shen, and Uthaiapon Tantipongpipat. Fast and memory efficient differentially private-SGD via JL projections. *Advances in Neural Information Processing Systems*, 34:19680–19691, 2021.

- [43] Zhiqi Bu, Jialin Mao, and Shiyun Xu. Scalable and efficient training of large convolutional neural networks with differential privacy. *Advances in Neural Information Processing Systems*, 35:38305–38318, 2022.
- [44] Zhiqi Bu, Yu-Xiang Wang, Sheng Zha, and George Karypis. Differentially private bias-term fine-tuning of foundation models. In *ICLR*, 2024.
- [45] Jie Fu, Qingqing Ye, Haibo Hu, Zhili Chen, Lulu Wang, Kuncan Wang, and Xun Ran. Dpsur: accelerating differentially private stochastic gradient descent using selective update and release. *arXiv preprint arXiv:2311.14056*, 2023.
- [46] Minxin Du, Xiang Yue, Sherman SM Chow, Tianhao Wang, Chenyu Huang, and Huan Sun. Dp-forward: Fine-tuning and inference on language models with differential privacy in forward pass. In *Proceedings of the 2023 ACM SIGSAC Conference on Computer and Communications Security*, pages 2665–2679, 2023.
- [47] Yaodong Yu, Maziar Sanjabi, Yi Ma, Kamalika Chaudhuri, and Chuan Guo. Vip: A differentially private foundation model for computer vision. *arXiv preprint arXiv:2306.08842*, 2023.
- [48] Yu-Xiang Wang, Borja Balle, and Shiva Prasad Kasiviswanathan. Sub-sampled rényi differential privacy and analytical moments accountant. In *The 22nd International Conference on Artificial Intelligence and Statistics*, pages 1226–1235. PMLR, 2019.
- [49] Qin Yang, Nicholas Stout, Meisam Mohammady, Han Wang, Ayesha Samreen, Christopher J. Quinn, Yan Yan, Ashish Kundu, and Yuan Hong. Plrv-o: Advancing differentially private deep learning via privacy loss random variable optimization. In *Proceedings of the 2025 ACM SIGSAC Conference on Computer and Communications Security, CCS '25*, page 306–320, New York, NY, USA, 2025. Association for Computing Machinery.
- [50] Shuainan Liu, Tianxi Ji, Zhongshuo Fang, Lu Wei, and Pan Li. Privacy loss of noise perturbation via concentration analysis of a product measure. In *SIGMOD*, 2026.
- [51] Quan Geng and Pramod Viswanath. The optimal mechanism in differential privacy. In *2014 IEEE International Symposium on Information Theory*, pages 2371–2375, 2014.
- [52] David Sommer, Sebastian Meiser, and Esfandiar Mohammadi. Privacy loss classes: The central limit theorem in differential privacy. *Cryptology ePrint Archive*, 2018.
- [53] Zhiqi Bu, Yu-Xiang Wang, Sheng Zha, and George Karypis. Differentially private optimization on large model at small cost. In *ICLR*, pages 3192–3218, 2023.
- [54] Aditya Golatkar, Alessandro Achille, Yu-Xiang Wang, Aaron Roth, Michael Kearns, and Stefano Soatto. Mixed differential privacy in computer vision. In *Proceedings of the IEEE/CVF Conference on Computer Vision and Pattern Recognition*, pages 8376–8386, 2022.
- [55] Zelun Luo, Yuliang Zou, Yijin Yang, Zane Durante, De-An Huang, Zhiding Yu, Chaowei Xiao, Li Fei-Fei, and Animashree Anandkumar. Differentially private video activity recognition. In *Proceedings of the IEEE/CVF Winter Conference on Applications of Computer Vision (WACV)*, pages 6657–6667, January 2024.
- [56] Qinqing Zheng, Jinshuo Dong, Qi Long, and Weijie Su. Sharp composition bounds for gaussian differential privacy via edgeworth expansion. In *International Conference on Machine Learning*, pages 11420–11435. PMLR, 2020.
- [57] Wael Alghamdi, Juan Felipe Gomez, Shahab Asoodeh, Flavio P. Calmon, Oliver Kosut, and Lalitha Sankar. The saddle-point method in differential privacy. In *Proceedings of the 40th International Conference on Machine Learning, ICML'23*. JMLR.org, 2023.
- [58] Jeremy Bernstein, Jiawei Zhao, Kamyar Azizzadenesheli, and Anima Anandkumar. signsgd with majority vote is communication efficient and fault tolerant. *arXiv preprint arXiv:1810.05291*, 2018.
- [59] Jonggyu Jang, Seongjin Hwang, and Hyun Jong Yang. Rethinking DP-SGD in discrete domain: Exploring logistic distribution in the realm of signSGD. In *Forty-first International Conference on Machine Learning*, 2024.
- [60] Erik Daxberger, Agustinus Kristiadi, Alexander Immer, Runa Eschenhagen, Matthias Bauer, and Philipp Hennig. Laplace redux-effortless bayesian deep learning. *Advances in neural information processing systems*, 34:20089–20103, 2021.
- [61] Nicolas Papernot, Abhradeep Thakurta, Shuang Song, Steve Chien, and Úlfar Erlingsson. Tempered sigmoid activations for deep learning with differential privacy. In *AAAI*, volume 35, pages 9312–9321, 2021.
- [62] Soham De, Leonard Berrada, Jamie Hayes, Samuel L Smith, and Borja Balle. Unlocking high-accuracy differentially private image classification through scale. *arXiv preprint arXiv:2204.13650*, 2022.
- [63] Qiaoyue Tang and Mathias Lécuyer. Dp-adam: Correcting dp bias in adam’s second moment estimation. In *ICLR 2023 Workshop on Trustworthy and Reliable Large-Scale Machine Learning Models*.
- [64] Badi Ghazi, Pasin Manurangsi, Pritish Kamath, Ravi Kumar Ravikumar, and Vadym Doroshenko. Connect the dots: Tighter discrete approximations of privacy loss distributions. In *PETS 2022*, 2022.
- [65] Ilya Mironov. Rényi differential privacy. In *2017 IEEE 30th computer security foundations symposium (CSF)*, pages 263–275. IEEE, 2017.
- [66] Issai Schur. Über eine klasse von mittelbildungen mit anwendungen auf die determinantentheorie. *Sitzungsberichte der Berliner Mathematischen Gesellschaft*, 22(9-20):51, 1923.
- [67] Godfrey H Hardy. Some simple inequalities satisfied by convex functions. *Messenger Math.*, 58:145–152, 1929.

## APPENDIX A OMITTED PROOFS

### A. Proof of Theorem III.2

In the following, we prove a tight bound on the moments accountant function of uni-variate Laplace mechanisms, as stated in Theorem III.2.

*Proof.* Consider two adjacent data sets  $d$  and  $d'$ . Without loss of generality suppose  $d'$  has an extra training sample. Let  $\zeta$  denote a fixed sampling rate. Consider any sampling realization over  $d \cup d' = d'$  using iid sampling with per element selection of  $\zeta$ .

With probability  $1 - \zeta$ , the extra sample in  $d'$  will not be included and thus query values over the sub-sampled datasets will be identical. Let  $\mu_0$  denote the resulting density of the Laplace mechanism in this case. Let  $q(d, \zeta)$  denote the mean of  $\mu_0$ . By construction  $|q(d, \zeta)| \leq C$ . With probability  $\zeta$ , the extra sample in  $d'$  will be kept resulting in different query values between the two data sets. Let  $\mu_1$  denote the resulting density of the Laplace mechanism of the query over the sub-sampled  $d'$ . Let  $q(d', \zeta)$  denote the mean of  $\mu_1$ . By construction  $|q(d', \zeta)| \leq C$ .

Thus, we can identify the mechanism over  $d'$  as having a mixture distribution,

$$M_q(d, \zeta) \sim \mu_0, \quad M_q(d', \zeta) \sim \mu \triangleq (1 - \zeta)\mu_0 + \zeta\mu_1.$$

For any  $\lambda$ , we aim to show:

$$A = \mathbb{E}_{z \sim \mu} \left[ \left( \frac{\mu(z)}{\mu_0(z)} \right)^\lambda \right] \leq \alpha, \quad \text{and} \quad B = \mathbb{E}_{z \sim \mu_0} \left[ \left( \frac{\mu_0(z)}{\mu(z)} \right)^\lambda \right] \leq \alpha.$$

for some explicit  $\alpha$  to be determined later.

Multiplying by  $\mu_0(z)/\mu_0(z)$  and rearranging, we can express:

$$A = \mathbb{E}_{z \sim \mu_0} \left[ \left( \frac{\mu(z)}{\mu_0(z)} \right)^{\lambda+1} \right] = \mathbb{E}_{z \sim \mu_0} \left[ \left( 1 - \zeta + \zeta \frac{\mu_1(z)}{\mu_0(z)} \right)^{\lambda+1} \right],$$

and

$$\begin{aligned} B &= \mathbb{E}_{z \sim \mu_0} \left[ \left( \frac{\mu_0(z)}{(1 - \zeta)\mu_0(z) + \zeta\mu_1(z)} \right)^\lambda \right] \\ &= \mathbb{E}_{z \sim \mu_0} \left[ \left( \frac{1}{1 - \zeta + \zeta \frac{\mu_1(z)}{\mu_0(z)}} \right)^\lambda \right]. \end{aligned}$$

Mironov et al. [13] (Section 3.1) demonstrate that  $A \geq B$  holds in general for centrally symmetric distributions.

We thus focus on analyzing  $A$ . We start by applying the binomial theorem and linearity of expectation,

$$\begin{aligned} A &= \mathbb{E}_{z \sim \mu_0} \left[ \left( 1 - \zeta + \zeta \frac{\mu_1(z)}{\mu_0(z)} \right)^{\lambda+1} \right] \\ &= \mathbb{E}_{z \sim \mu_0} \left[ \sum_{\eta=0}^{\lambda+1} \binom{\lambda+1}{\eta} (1-\zeta)^{\lambda+1-\eta} \zeta^\eta \left( \frac{\mu_1(z)}{\mu_0(z)} \right)^\eta \right] \\ &= \sum_{\eta=0}^{\lambda+1} \binom{\lambda+1}{\eta} (1-\zeta)^{\lambda+1-\eta} \zeta^\eta \mathbb{E}_{z \sim \mu_0} \left[ \left( \frac{\mu_1(z)}{\mu_0(z)} \right)^\eta \right]. \end{aligned}$$

We can simplify the ratio of the densities as

$$\begin{aligned} \frac{\mu_1(z)}{\mu_0(z)} &= \frac{\frac{1}{2b} \exp(-\frac{|z-q(d',\zeta)|}{b})}{\frac{1}{2b} \exp(-\frac{|z-q(d,\zeta)|}{b})} \\ &= \exp\left(\frac{1}{b} (|z-q(d,\zeta)| - |z-q(d',\zeta)|)\right). \end{aligned}$$

Without loss of generality, consider that  $q(d,\zeta) < q(d',\zeta)$ . We split up the real line into three intervals:  $\mathbb{R} = (-\infty, q(d,\zeta)] \cup (q(d,\zeta), q(d',\zeta)) \cup [q(d',\zeta), \infty)$ .

We evaluate the expectation  $\mathbb{E}_{z \sim \mu_0} \left[ \left( \frac{\mu_1(z)}{\mu_0(z)} \right)^\eta \right]$  over these three intervals separately (conditionally) and then will combine them afterwards (with probabilities of respective events occurring). We will analyze the middle interval last.

*Case A1:*  $z < q(d,\zeta)$ :: Since  $z < q(d,\zeta)$ ,  $|z-q(d,\zeta)| = q(d,\zeta) - z$ . Likewise,  $z < q(d',\zeta)$ , so  $|z-q(d',\zeta)| = q(d',\zeta) - z$ . The likelihood ratio simplifies

$$\begin{aligned} \frac{\mu_1(z)}{\mu_0(z)} &= \exp\left(\frac{1}{b} (|z-q(d,\zeta)| - |z-q(d',\zeta)|)\right) \\ &= \exp\left(\frac{1}{b} (q(d,\zeta) - z - (q(d',\zeta) - z))\right) \\ &= \exp\left(\frac{1}{b} (q(d,\zeta) - q(d',\zeta))\right). \end{aligned}$$

We observe there is no dependence on  $z$ , so this ratio becomes a constant in the expectation. Under  $\mu_0$ ,  $z$  is equally distributed about  $q(d,\zeta)$ . So the probability of this event is  $1/2$ . Thus, the contribution to the total expectation is

$$\frac{1}{2} \exp\left(\frac{\eta}{b} (q(d,\zeta) - q(d',\zeta))\right).$$

*Case A2:*  $z > q(d',\zeta)$ :: Since  $z > q(d',\zeta)$ ,  $|z-q(d',\zeta)| = z - q(d',\zeta)$ . Likewise,  $z > q(d,\zeta)$ , so  $|z-q(d,\zeta)| = z - q(d,\zeta)$ . The likelihood ratio simplifies

$$\begin{aligned} \frac{\mu_1(z)}{\mu_0(z)} &= \exp\left(\frac{1}{b} (|z-q(d,\zeta)| - |z-q(d',\zeta)|)\right) \\ &= \exp\left(\frac{1}{b} (z - q(d,\zeta) - (z - q(d',\zeta)))\right) \\ &= \exp\left(\frac{1}{b} (q(d',\zeta) - q(d,\zeta))\right). \end{aligned}$$

Again, the ratio is a constant with respect to  $z$ . The probability of the event is more complicated to analyze than the previous event.

$$\begin{aligned} &\int_{q(d',\zeta)}^{\infty} \frac{1}{2b} \exp(-\frac{|z-q(d,\zeta)|}{b}) db \\ &= \int_{q(d',\zeta)}^{\infty} \frac{1}{2b} \exp(-\frac{z-q(d,\zeta)}{b}) db \\ &= \frac{1}{2b} \exp(\frac{q(d,\zeta)}{b}) \int_{q(d',\zeta)}^{\infty} \exp(-\frac{z}{b}) db \\ &= \frac{1}{2b} \exp(\frac{q(d,\zeta)}{b}) \frac{1}{-\frac{1}{b}} \exp(-\frac{z}{b}) \Big|_{q(d',\zeta)}^{\infty} \\ &= \frac{1}{2} \exp(\frac{q(d,\zeta)}{b}) \exp(-\frac{q(d',\zeta)}{b}) \\ &= \frac{1}{2} \exp(\frac{q(d,\zeta) - q(d',\zeta)}{b}) \end{aligned}$$

Thus, the contribution to the total expectation is

$$\begin{aligned} &\frac{1}{2} \exp(\frac{q(d,\zeta) - q(d',\zeta)}{b}) \exp\left(\frac{\eta}{b} (q(d',\zeta) - q(d,\zeta))\right) \\ &= \frac{1}{2} \exp\left(\frac{\eta-1}{b} (q(d',\zeta) - q(d,\zeta))\right). \end{aligned}$$

*Case A3:*  $q(d,\zeta) \leq z \leq q(d',\zeta)$ :: Since  $z > q(d,\zeta)$ ,  $|z-q(d,\zeta)| = z - q(d,\zeta)$ . Since  $z < q(d',\zeta)$ , so  $|z-q(d',\zeta)| = q(d',\zeta) - z$ . The likelihood ratio simplifies

$$\begin{aligned} \frac{\mu_1(z)}{\mu_0(z)} &= \exp\left(\frac{1}{b} (|z-q(d,\zeta)| - |z-q(d',\zeta)|)\right) \\ &= \exp\left(\frac{1}{b} (z - q(d,\zeta) - (q(d',\zeta) - z))\right) \\ &= \exp\left(\frac{1}{b} (-q(d,\zeta) - q(d',\zeta) + 2z)\right). \end{aligned}$$

Plugging this back into the expectation,

$$\begin{aligned} &\mathbb{E}_{z \sim \mu_0} \left[ \left( \frac{\mu_1(z)}{\mu_0(z)} \right)^\eta \right] \\ &= \mathbb{E}_{z \sim \mu_0} \left[ \exp\left(\frac{\eta}{b} (-q(d,\zeta) - q(d',\zeta) + 2z)\right) \right] \\ &= \exp\left(\frac{\eta}{b} (-q(d,\zeta) - q(d',\zeta))\right) \\ &\quad \times \mathbb{E}_{z \sim \mu_0} \left[ \exp\left(\frac{2\eta z}{b}\right) \right]. \end{aligned}$$

Evaluating the inner expectation (only over the interval for

this case),

$$\begin{aligned}
& \mathbb{E}_{z \sim \mu_0} \left[ \exp \left( \frac{2\eta z}{b} \right) \right] \\
&= \int_{q(d, \zeta)}^{q(d', \zeta)} \frac{1}{2b} \exp \left( -\frac{|z - q(d, \zeta)|}{b} + \frac{2\eta z}{b} \right) db \\
&= \frac{1}{2b} \exp \left( \frac{q(d, \zeta)}{b} \right) \int_{q(d, \zeta)}^{q(d', \zeta)} \exp \left( z \left( -\frac{1 - 2\eta}{b} \right) \right) db \\
&= \frac{1}{2b} \exp \left( \frac{q(d, \zeta)}{b} \right) \frac{b}{2\eta - 1} \left[ \exp \left( q(d', \zeta) \left( -\frac{1 - 2\eta}{b} \right) \right) \right. \\
&\quad \left. - \exp \left( q(d, \zeta) \left( -\frac{1 - 2\eta}{b} \right) \right) \right] \\
&= \frac{1}{2(2\eta - 1)} \left[ \exp \left( q(d', \zeta) \frac{2\eta - 1}{b} + q(d, \zeta) \frac{1}{b} \right) \right. \\
&\quad \left. - \exp \left( q(d, \zeta) \frac{2\eta}{b} \right) \right].
\end{aligned}$$

Thus, the contribution to the expectation from this case is

$$\begin{aligned}
\mathbb{E}_{z \sim \mu_0} \left[ \left( \frac{\mu_1(z)}{\mu_0(z)} \right)^\eta \right] &= \exp \left( \frac{\eta}{b} (-q(d, \zeta) - q(d', \zeta)) \right) \\
&\quad \times \frac{1}{2(2\eta - 1)} \left[ \exp \left( q(d', \zeta) \frac{2\eta - 1}{b} \right. \right. \\
&\quad \left. \left. + q(d, \zeta) \frac{1}{b} \right) - \exp \left( q(d, \zeta) \frac{2\eta}{b} \right) \right].
\end{aligned}$$

*Combining Cases A1-A3::* Combining the results, we have that

$$\begin{aligned}
A &= \mathbb{E}_{z \sim \mu_0} \left[ \left( \frac{\mu(z)}{\mu_0(z)} \right)^{\lambda+1} \right] \\
&= \frac{1}{2} \exp \left( \frac{\eta}{b} (q(d, \zeta) - q(d', \zeta)) \right) \\
&\quad + \frac{1}{2} \exp \left( \frac{\eta - 1}{b} (q(d', \zeta) - q(d, \zeta)) \right) \\
&\quad + \exp \left( \frac{\eta}{b} (-q(d, \zeta) - q(d', \zeta)) \right) \\
&\quad \times \frac{1}{2(2\eta - 1)} \left[ \exp \left( q(d', \zeta) \frac{2\eta - 1}{b} + q(d, \zeta) \frac{1}{b} \right) \right. \\
&\quad \left. - \exp \left( q(d, \zeta) \frac{2\eta}{b} \right) \right]
\end{aligned}$$

Recall that the query values over the sub-sampled data sets  $q(d, \zeta)$  and  $q(d', \zeta)$  are averaged over the queries (gradients) of the included samples, so the effect of a single sample is smaller the more samples are included. For simplicity, by inspection of the formula we consider a worst case bound using  $q(d) = 0$  and  $q(d', \zeta) = C$ .

$$\begin{aligned}
A &= \frac{1}{2} \exp \left( \frac{-\eta C}{b} \right) \\
&\quad + \frac{1}{2} \exp \left( \frac{(\eta - 1)C}{b} \right) \\
&\quad + \exp \left( \frac{-\eta C}{b} \right) \frac{1}{2(2\eta - 1)} \left[ \exp \left( \frac{(\eta - 1)C}{b} \right) - \exp(0) \right] \\
&= \exp \left( \frac{-\eta C}{b} \right) \left[ \frac{1}{2} - \frac{1}{2(2\eta - 1)} \right] \\
&\quad + \exp \left( \frac{(\eta - 1)C}{b} \right) \left[ \frac{1}{2} + \frac{1}{2(2\eta - 1)} \right] \\
&= \exp \left( \frac{-\eta C}{b} \right) \left[ \frac{\eta - 1}{2\eta - 1} \right] + \exp \left( \frac{(\eta - 1)C}{b} \right) \left[ \frac{\eta}{2\eta - 1} \right]. \tag{A.1}
\end{aligned}$$

**Analysis for B:** Following the argument in Proof A-A (Theorem 3.2), and using binomial expansion with term-wise comparison, we find that  $B \geq A$ , consistent with the result of Mironov et al.  $\square$

## B. Proof of Theorem III.5

In the following, we prove Theorem III.5, that the moments accounting function of the uni-variate Laplace mechanism is Schur-convex. We first prove the following technical lemma, involving second derivatives of the MAF, before continuing on to the main proof.

**Lemma A.1.** *The second derivative of the moments accountant function  $\alpha(\lambda)$  in Theorem III.2 with respect to the marginal clipped gradients  $|\mathbf{g}_i|$  is non-negative.*

*Proof.* Let  $a_\eta = \binom{\lambda+1}{\eta} (1 - \zeta)^{\lambda+1 - \eta} \zeta^\eta$  be the positive weight associated with each  $\eta$ . The second derivative of  $\alpha(\lambda)$  can be written as

$$\frac{d^2 \alpha(\lambda)}{d|\mathbf{g}_i|^2} = \frac{\left( \sum_\eta a_\eta F(|\mathbf{g}_i|, \eta) \right) \left( \sum_\eta a_\eta \frac{d^2 F}{d|\mathbf{g}_i|^2} \right) - \left( \sum_\eta a_\eta \frac{dF}{d|\mathbf{g}_i|} \right)^2}{\left( \sum_\eta a_\eta F(|\mathbf{g}_i|, \eta) \right)^2}.$$

Recall:

$$\begin{aligned}
F(|\mathbf{g}_i|, \eta) &= \frac{\eta}{2\eta - 1} e^{\frac{(\eta-1)|\mathbf{g}_i|}{b}} + \frac{\eta - 1}{2\eta - 1} e^{-\frac{\eta|\mathbf{g}_i|}{b}}, \\
\frac{dF}{d|\mathbf{g}_i|} &= \frac{\eta(\eta - 1)}{b(2\eta - 1)} \left( e^{\frac{(\eta-1)|\mathbf{g}_i|}{b}} - e^{-\frac{\eta|\mathbf{g}_i|}{b}} \right), \\
\frac{d^2 F}{d|\mathbf{g}_i|^2} &= \frac{\eta(\eta - 1)}{b^2(2\eta - 1)} \left( (\eta - 1) e^{\frac{(\eta-1)|\mathbf{g}_i|}{b}} + \eta e^{-\frac{\eta|\mathbf{g}_i|}{b}} \right).
\end{aligned}$$

Expand  $F \times F''$ :

$$\begin{aligned} F \times F'' &= \left( \frac{\eta}{2\eta-1} e^{\frac{(\eta-1)|\mathbf{g}_i|}{b}} + \frac{\eta-1}{2\eta-1} e^{-\frac{\eta|\mathbf{g}_i|}{b}} \right) \\ &\quad \times \frac{\eta(\eta-1)}{b^2(2\eta-1)} \left( (\eta-1)e^{\frac{(\eta-1)|\mathbf{g}_i|}{b}} + \eta e^{-\frac{\eta|\mathbf{g}_i|}{b}} \right) \\ &= \frac{\eta(\eta-1)}{b^2(2\eta-1)^2} \left[ \eta(\eta-1)e^{2\frac{(\eta-1)|\mathbf{g}_i|}{b}} + \eta^2 e^{\frac{(\eta-1)|\mathbf{g}_i|/b - \eta|\mathbf{g}_i|/b}{b}} \right. \\ &\quad \left. + (\eta-1)^2 e^{-\frac{\eta|\mathbf{g}_i|}{b} + \frac{(\eta-1)|\mathbf{g}_i|}{b}} + \eta(\eta-1)e^{-2\frac{\eta|\mathbf{g}_i|}{b}} \right]. \end{aligned}$$

Notice:

$$e^{\frac{(\eta-1)|\mathbf{g}_i|}{b}} e^{-\frac{\eta|\mathbf{g}_i|}{b}} = e^{-\frac{|\mathbf{g}_i|}{b}}, \quad e^{-\frac{\eta|\mathbf{g}_i|}{b}} e^{\frac{(\eta-1)|\mathbf{g}_i|}{b}} = e^{-\frac{|\mathbf{g}_i|}{b}}.$$

Thus:

$$\begin{aligned} F \times F'' &= \frac{\eta(\eta-1)}{b^2(2\eta-1)^2} \times \\ &\quad \left[ \eta(\eta-1)e^{2\frac{(\eta-1)|\mathbf{g}_i|}{b}} \right. \\ &\quad \left. + (\eta^2 + (\eta-1)^2)e^{-\frac{|\mathbf{g}_i|}{b}} + \eta(\eta-1)e^{-2\frac{\eta|\mathbf{g}_i|}{b}} \right]. \end{aligned}$$

Expand  $\left(\frac{dF}{d|\mathbf{g}_i|}\right)^2$ :

$$\begin{aligned} \left(\frac{dF}{d|\mathbf{g}_i|}\right)^2 &= \left(\frac{\eta(\eta-1)}{b(2\eta-1)}\right)^2 \left(e^{\frac{(\eta-1)|\mathbf{g}_i|}{b}} - e^{-\frac{\eta|\mathbf{g}_i|}{b}}\right)^2 \\ &= \left(\frac{\eta(\eta-1)}{b(2\eta-1)}\right)^2 \left(e^{2\frac{(\eta-1)|\mathbf{g}_i|}{b}} - 2e^{-\frac{|\mathbf{g}_i|}{b}} + e^{-2\frac{\eta|\mathbf{g}_i|}{b}}\right). \end{aligned}$$

Comparing individual terms pointwise shows that  $F \times F'' \geq (F')^2$  holds for all  $|\mathbf{g}_i| \geq 0$  and  $\eta \geq 0$ . Applying the Cauchy-Schwarz inequality to the positive sequence  $\{\sqrt{a_\eta} \sqrt{F(|\mathbf{g}_i|, \eta)}\}$  and  $\{\sqrt{a_\eta} \sqrt{d^2 F/d|\mathbf{g}_i|^2}\}$  yields

$$\left(\sum_{\eta} a_{\eta} \sqrt{F(|\mathbf{g}_i|, \eta)} \sqrt{\frac{d^2 F}{d|\mathbf{g}_i|^2}}\right)^2 \leq \left(\sum_{\eta} a_{\eta} F(|\mathbf{g}_i|, \eta)\right) \left(\sum_{\eta} a_{\eta} \frac{d^2 F}{d|\mathbf{g}_i|^2}\right). \quad (\text{A.2})$$

but since  $F \times F'' \geq (F')^2$ , pointwise, we have  $\sqrt{F(|\mathbf{g}_i|, \eta)} \sqrt{\frac{d^2 F}{d|\mathbf{g}_i|^2}} \geq \frac{dF}{d|\mathbf{g}_i|}$ . Hence,

$$\left(\sum_{\eta} a_{\eta} \frac{dF}{d|\mathbf{g}_i|}\right) \leq \left(\sum_{\eta} a_{\eta} \sqrt{F(|\mathbf{g}_i|, \eta)} \sqrt{\frac{d^2 F}{d|\mathbf{g}_i|^2}}\right).$$

The last two inequalities together yield:

$$\left(\sum_{\eta} a_{\eta} \frac{dF}{d|\mathbf{g}_i|}\right)^2 \leq \left(\sum_{\eta} a_{\eta} F(|\mathbf{g}_i|, \eta)\right) \left(\sum_{\eta} a_{\eta} \frac{d^2 F}{d|\mathbf{g}_i|^2}\right),$$

which shows the numerator is non-negative. Therefore,

$$\frac{d^2 \alpha(\lambda)}{d|\mathbf{g}_i|^2} \geq 0,$$

and  $\alpha(\lambda)$  is Schur-convex.  $\square$

We are now ready to prove Theorem III.5.

*Proof.* We apply Schur's condition (also known as the Schur–Strowski criterion) to prove that  $\alpha(\lambda)$  is Schur-convex. Recall that a symmetric function  $f(x_1, \dots, x_n)$  is Schur-convex if and only if for all  $i \neq j$ ,

$$(x_i - x_j) \left( \frac{\partial f}{\partial x_i} - \frac{\partial f}{\partial x_j} \right) \geq 0.$$

In our case, the function is  $\alpha(\lambda) = \sum_{i=1}^n \alpha_{\bar{\mathbf{g}}_i}(\lambda)$ , where  $\bar{\mathbf{g}}_i$  is the noisy version of the  $\ell_2$ -clipped marginal gradients. Denote by  $\mathbf{g}_i, i \in [n]$ , marginal gradients after  $\ell_2$  clipping and before the addition of DP noise. Then, with Theorem III.2, the uni-variate moments accountant for the  $i$ -th coordinate satisfies

$$\alpha_{\bar{\mathbf{g}}_i}(\lambda) \leq \log \left[ \sum_{\eta=0}^{\lambda+1} \binom{\lambda+1}{\eta} (1-\zeta)^{\lambda+1-\eta} \zeta^{\eta} F(|\mathbf{g}_i|, \eta) \right], \quad (\text{A.3})$$

where the function  $F(|\mathbf{g}_i|, \eta)$  is defined as

$$F(|\mathbf{g}_i|, \eta) = \frac{e^{\frac{(\eta-1)|\mathbf{g}_i|}{b}}}{2} + \frac{e^{-\frac{\eta|\mathbf{g}_i|}{b}}}{2} + \frac{e^{\frac{(\eta-1)|\mathbf{g}_i|}{b}} - e^{-\frac{\eta|\mathbf{g}_i|}{b}}}{2(2\eta-1)}. \quad (\text{A.4})$$

Define the term inside the square brackets in A.3 as  $X$ . Then, the derivative of  $\alpha_{\bar{\mathbf{g}}_i}(\lambda)$  with respect to  $|\mathbf{g}_i|$  satisfies

$$\frac{d\alpha_{\bar{\mathbf{g}}_i}(\lambda)}{d|\mathbf{g}_i|} = \frac{\sum_{\eta=0}^{\lambda+1} \binom{\lambda+1}{\eta} (1-\zeta)^{\lambda+1-\eta} \zeta^{\eta} \frac{dF}{d|\mathbf{g}_i|}}{X}. \quad (\text{A.5})$$

Lets compute the derivative  $\frac{dF}{d|\mathbf{g}_i|}$ :

$$\begin{aligned} \frac{dF}{d|\mathbf{g}_i|} &= \frac{(\eta-1)}{2b} e^{\frac{(\eta-1)|\mathbf{g}_i|}{b}} - \frac{\eta}{2b} e^{-\frac{\eta|\mathbf{g}_i|}{b}} \\ &\quad + \frac{1}{2(2\eta-1)} \left( \frac{(\eta-1)}{b} e^{\frac{(\eta-1)|\mathbf{g}_i|}{b}} + \frac{\eta}{b} e^{-\frac{\eta|\mathbf{g}_i|}{b}} \right). \end{aligned} \quad (\text{A.6})$$

Special cases:

- For  $\eta = 0$ , the terms cancel symmetrically and  $\frac{dF}{d|\mathbf{g}_i|} = 0$ .
- For  $\eta = 1$ , the derivative simplifies to 0 by symmetry.
- For  $\eta > 1$ , expanding and grouping terms, we have

$$\frac{dF}{d|\mathbf{g}_i|} = \frac{(\eta-1)\eta}{b(2\eta-1)} \left( e^{\frac{(\eta-1)|\mathbf{g}_i|}{b}} - e^{-\frac{\eta|\mathbf{g}_i|}{b}} \right). \quad (\text{A.7})$$

Since  $\eta > 1$ , the prefactor  $\frac{(\eta-1)\eta}{b(2\eta-1)}$  is positive. Moreover, for any  $|\mathbf{g}_i| \geq 0$ ,  $e^{\frac{(\eta-1)|\mathbf{g}_i|}{b}} \geq e^{-\frac{\eta|\mathbf{g}_i|}{b}}$ . Thus,  $\frac{dF}{d|\mathbf{g}_i|} \geq 0$  for all  $\mathbf{g}_i$  and all  $\eta$ .

As stated earlier,

$$\frac{d\alpha_{\bar{\mathbf{g}}_i}(\lambda)}{d|\mathbf{g}_i|} = \frac{\sum_{\eta=0}^{\lambda+1} \binom{\lambda+1}{\eta} (1-\zeta)^{\lambda+1-\eta} \zeta^{\eta} \frac{dF}{d|\mathbf{g}_i|}}{X}.$$

Since each  $\frac{dF}{d|\mathbf{g}_i|} \geq 0$ ,  $X > 0$ , and all the coefficients are positive, it follows that

$$\frac{\partial \alpha(\lambda)}{\partial |\mathbf{g}_i|} \geq 0.$$

Since  $\alpha(\lambda) = \sum_{i=1}^n \alpha_{\bar{\mathbf{g}}_i}(\lambda)$  with each  $\alpha_{\bar{\mathbf{g}}_i}(\lambda)$  depending only on  $|\mathbf{g}_i|$ , we have  $\frac{\partial \alpha(\lambda)}{\partial |\mathbf{g}_i|} = \frac{d\alpha_{\bar{\mathbf{g}}_i}(\lambda)}{d|\mathbf{g}_i|}$ . Thus, the overall

moments accountant function (MAF) is non-decreasing. To satisfy the Schur–Ostrowski criterion, it suffices to show that the second derivative of  $\alpha(\lambda)$  is non-negative (MAF is convex). A positive second derivative ensures that for any  $i \neq j$ , both  $|\mathbf{g}_i| - |\mathbf{g}_j|$  and  $\frac{\partial \alpha(\lambda)}{\partial |\mathbf{g}_i|} - \frac{\partial \alpha(\lambda)}{\partial |\mathbf{g}_j|}$  share the same sign, thereby satisfying the criterion. In Theorem A.1 we proved that the second derivatives are non-negative, concluding the proof for Theorem III.5.  $\square$   $\square$

An *alternative* approach is to prove the Schur-convexity of the univariate MAF and apply the following results.

**Proposition A.2** (Schur [66]; Hardy–Littlewood–Pólya [67]). *Let  $I \subset \mathbb{R}$  be an interval and  $g : I \rightarrow \mathbb{R}$  be a convex function. Then the function*

$$\varphi(x) = \sum_{i=1}^n g(x_i)$$

is Schur-convex on  $I^n$ . Consequently, if  $x \prec y$  on  $I^n$ , then

$$\varphi(x) \leq \varphi(y).$$

### C. Proof of Theorem III.6

In the following, we prove Lemma III.6 on the majorization set for  $\ell_2$  clipped gradients.

*Proof.* Since the  $\ell_2$  clipping ensures that  $\|\mathbf{g}\|_2 \leq C$ , we have  $|\mathbf{g}_1| \leq C = x_1$ . Applying the AM–QM inequality to the first  $i$  marginal clipped gradients, we have

$$\frac{1}{i} \sum_{j=1}^i |\mathbf{g}_j| \leq \sqrt{\frac{1}{i} \sum_{j=1}^i (|\mathbf{g}_j|)^2} \leq \frac{C}{\sqrt{i}},$$

which implies

$$\sum_{j=1}^i |\mathbf{g}_j| \leq C\sqrt{i}.$$

On the other hand, the majorization set  $x$  satisfies

$$\sum_{j=1}^i x_j = C\sqrt{i},$$

since

$$\sum_{j=1}^i x_j = C(\sqrt{i} - \sqrt{0})$$

by telescoping the differences. Thus, for each  $i = 1, \dots, n$ , we have

$$\sum_{j=1}^i |\mathbf{g}_j| \leq \sum_{j=1}^i x_j,$$

establishing that  $|\mathbf{G}| \prec_w x$ .  $\square$

---

## Algorithm 2 LAP<sub>2</sub> DP-SGD: Drop-in Replacement of Gaussian DP-SGD

---

**Input:** Dataset  $\mathcal{D}$ , steps  $T$ , sampling rate  $\zeta$ , learning rate  $\eta$ , target privacy  $(\epsilon, \delta)$

**Output:** Final model parameters  $\theta$  under  $(\epsilon, \delta)$ -DP

// **Step 1: Optimize**  $(C, b)$  **using Algorithm 1**

$(C, b) \leftarrow \mathcal{H}(\epsilon, \delta, T, \zeta)$

// **Step 2: DP-SGD with  $\ell_2$  clipping and Laplace noise**

**for**  $t = 1$  **to**  $T$  **do**

  Sample mini-batch  $\mathcal{B}_t \subset \mathcal{D}$  at rate  $\zeta$

**for each**  $(x_i, y_i) \in \mathcal{B}_t$  **do**

    Compute per-example gradient:  $\mathbf{g}_i = \nabla \ell(f_{\theta}(x_i), y_i)$

    Clip:  $\mathbf{g}_i^C = \frac{\mathbf{g}_i}{\max(1, \|\mathbf{g}_i\|_2/C)}$

**end for**

  Average:  $\bar{\mathbf{g}}_t = \frac{1}{|\mathcal{B}_t|} \sum \mathbf{g}_i^C$

  Add noise:  $\tilde{\mathbf{g}}_t = \bar{\mathbf{g}}_t + \text{Lap}(0, b)$

  Update model:  $\theta \leftarrow \theta - \eta \cdot \text{Optimizer}(\tilde{\mathbf{g}}_t)$

**end for**

**return**  $\theta$

---

## APPENDIX B

### FURTHER ANALYSIS OF LAP<sub>2</sub> DP-SGD

The LAP<sub>2</sub> DP-SGD algorithm (Algorithm 2) serves as a drop-in replacement for Gaussian DP-SGD. Leveraging our majorization-based accountant, it provides tight  $(\epsilon, \delta)$  guarantees while preserving training efficiency. We examine the evolution of DP moments under LAP<sub>2</sub> and analyze its batching and scaling behavior, highlighting how privacy and utility evolve across different regimes of  $\epsilon$ .

#### A. Evolution of Lap<sub>2</sub> Moments: A Case Study

We first in Figure 9 illustrate the relationship between the clipping threshold and the privacy budget  $\epsilon$  under the LAP<sub>2</sub> mechanism for two privacy regimes. Figure 9a corresponds to the tight-privacy region ( $\epsilon \in [0, 1]$ ), while Figure 9b represents the moderate-privacy region ( $\epsilon \in [1, 5]$ ). The color bar indicates the optimal moment order  $\lambda_{best}$  obtained from the accountant. As shown, smaller clipping values dominate in the high-privacy regime, where higher  $\lambda_{best}$  values are exploited for tighter accounting. In contrast, as  $\epsilon$  increases, larger clipping thresholds become feasible with smaller optimal  $\lambda_{best}$ , reflecting improved stability and reduced noise requirements in moderate-privacy settings.

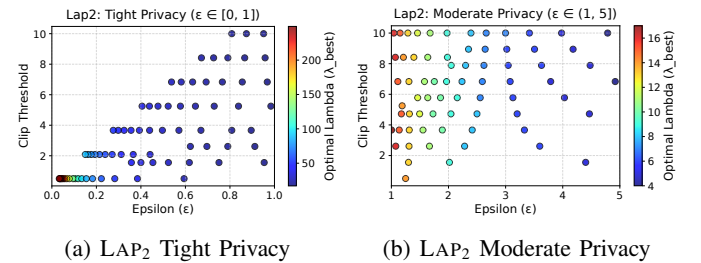


Fig. 9: LAP<sub>2</sub> supports larger clipping norms without runaway noise, due to its heavy tails and efficient high-order moments accounting.

### B. Scaling Laws under Lap<sub>2</sub>

Previous works [14] have found scaling laws, correlations between the various parameters as well as the accuracy of the final differentially private model, for the gaussian noise mechanism. These scaling laws are also applicable to the Lap<sub>2</sub> noise mechanism. Many of these laws are derived in the discussion of SNR in Section III, but an important scaling law is the relationship between accuracy and batch size. Under the gaussian mechanism, it was found that accuracy decreases as batch size increases, falling very slowly for datasets like CIFAR10. In Figure 10, it is shown that Lap<sub>2</sub> has a peak batch size for CIFAR10, after which the accuracy decays slowly. In Figure 11, the accuracy decreases log linearly as batch size increases for fixed clip,  $\epsilon$  and epochs.

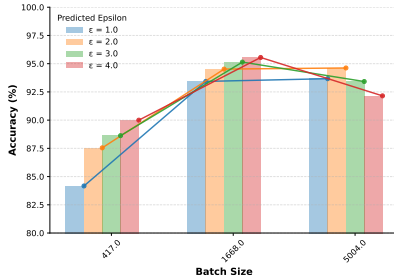


Fig. 10: Accuracy vs batch size for various  $\epsilon$ . Found by fine-tuning a ViT with CIFAR10 trained for 1 epoch. This graph shows that there is an optimal batch size, with a slow decay in accuracy afterward. Under gaussian, the decay is slow and consistent across batch sizes[14].

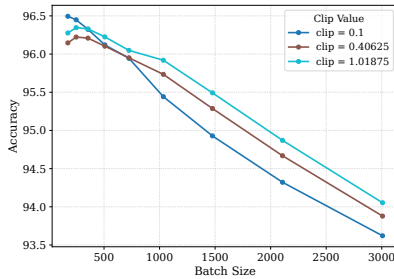


Fig. 11: Accuracy vs batch size for various clipping norms on the MNIST dataset trained on CNN using LAP<sub>2</sub>-DPSGD for 20 epochs for a fixed privacy budget  $\epsilon = 2$  and  $\delta = 10^{-5}$ .